Review

Not peer-reviewed version

# Nanomaterial-Enabled Spectroscopic Sensing: Building a New Paradigm for Precision Detection of Pesticide Residues

Wang Mei * , Niu Yue , Peng Hao , Zhang PengCheng , Bu Quan , Song Xianghai * , Yuan Shouqi

Posted Date: 22 September 2025

doi: 10.20944/preprints202509.1694.v1

Keywords: spectroscopic techniques; nanomaterials; pesticide residue detection; SERS; hyperspectral imaging

*Review*

# Nanomaterial-Enabled Spectroscopic Sensing: Building a New Paradigm for Precision Detection of Pesticide Residues

**Mei Wang [1,*], Yue Niu [1], Hao Peng [1], PengCheng Zhang [1], Quan Bu [1], Xianghai Song [2,*] and Shouqi Yuan [3]**

[1] School of Agricultural Engineering, Jiangsu University, Zhenjiang 212013, China
[2] Institute of the Green Chemistry and Chemical Technology, School of Chemistry and Chemical Engineering, Jiangsu University, Zhenjiang 212013, China
[3] Research Center of Fluid Machinery Engineering and Technology, Jiangsu University, Zhenjiang 212013, China
* Correspondence: 1000004927@ujs.edu.cn (M.W.); songxianghai@ujs.edu.cn (X.S.)

## Abstract

This review summarizes the application of spectroscopic techniques in pesticide residue analysis, with a focus on the principles, advancements, and challenges of surface-enhanced Raman spectroscopy (SERS), infrared spectroscopy, fluorescence spectroscopy, ultraviolet-visible (UV-Vis) spectroscopy, and hyperspectral imaging (HSI). Nanomaterials, serving as key enhancing substrates, significantly improve the sensitivity and selectivity of these detection methods. The article critically evaluates the strengths and limitations of each technique in practical applications—such as the exceptional sensitivity of SERS versus its dependence on substrate reproducibility, and the non-destructive nature of hyperspectral imaging against the complexity of data processing. Future research directions should emphasize the development of intelligent nanosubstrates, the construction of cross-modal spectral databases, and the miniaturization of integrated spectroscopic-mass spectrometric instruments. These advancements are essential for enhancing the efficiency and reliability of agricultural and food safety monitoring.

**Keywords:** spectroscopic techniques; nanomaterials; pesticide residue detection; SERS; hyperspectral imaging

---

## 1. Introduction

Pesticides, as a critical technological tool for ensuring food security, have long been at the center of debate in agricultural science due to their dual nature—offering significant benefits while posing potential risks [1]. In practical agricultural production, pesticides play a vital role in controlling pests and diseases and suppressing weeds, thereby substantially increasing crop yields [2–4]. According to the Food and Agriculture Organization (FAO) of the United Nations, discontinuing pesticide use globally could result in annual crop losses exceeding 30%, with some cash crops facing complete failure. Beyond yield protection, pesticides also reduce post-harvest losses and improve the visual quality of produce, thus supporting the large-scale, mechanized development of modern agriculture [5,6]. Herbicides, for example, have dramatically simplified field management, significantly boosting agricultural efficiency. However, the issue of pesticide residues has become increasingly prominent. Residual chemicals in food products can accumulate through the food chain, posing potential threats to both ecosystems and human health—particularly in fresh produce, where minimal processing heightens exposure risks [7,8]. To address this challenge, international regulatory frameworks have been established, centered on Maximum Residue Limits (MRLs), and implemented through comprehensive measures including controlled pesticide development, mandated pre-harvest intervals, and rigorous monitoring throughout the supply chain [9]. In China, innovative initiatives such as technology outreach programs for agribusinesses and farmer training in proper pesticide use aim to reduce over-application at the source, while green solutions like biodegradation technologies are being actively explored. Against this backdrop, achieving a scientific balance between agricultural productivity and ecological safety has emerged as a key challenge in advancing sustainable agriculture [10].

Pesticide residue detection stands as a critical line of defense in food safety, with the sophistication of detection methods directly influencing regulatory effectiveness [11–13]. Conventional techniques such as chromatography and mass spectrometry (MS), while highly accurate, face practical limitations including high equipment costs, complex sample preparation, and lengthy analysis times [14–16]. In contrast, spectroscopic technologies are reshaping the landscape of residue detection by offering non-destructive, rapid, and in-situ analysis capabilities [17,18]. For instance, Raman spectroscopy enables on-site screening within two minutes, shifting regulatory approaches from reactive traceability to proactive interception. Aqueous-phase detection systems eliminate the need for toxic solvents, aligning with the principles of green chemistry. Notably, gold nanoparticle-enhanced Raman spectroscopy (SERS) achieves detection limits as low as 0.1 ppb, and when combined with hyperspectral imaging (HSI) and artificial intelligence (AI) algorithms, can precisely map the spatial distribution of residues. These technological advances are transforming spectroscopic methods from supplementary tools into core solutions in the industry.

Owing to their unique analytical principles, spectroscopic techniques demonstrate clear advantages across multiple dimensions. They not only overcome the limitations of traditional methods but also continuously expand application frontiers through innovation, driving a revolutionary shift in modern analytical science [19]. In terms of analytical performance, spectroscopy offers three key strengths: non-contact measurement, ultra-high sensitivity, and the ability to detect multiple components simultaneously. Unlike conventional methods requiring extensive sample preparation, spectroscopic analysis allows for real-time, dynamic monitoring. Its distinctive "molecular fingerprint" identification—such as characteristic Raman peaks—proves particularly effective in detecting trace substances and analyzing complex matrices [20]. With advances in miniaturization, spectroscopic instruments are becoming increasingly portable and intelligent, opening new possibilities for rapid on-site testing [21,22].

These advantages are evident in four key areas:

(1) Non-destructive analysis: Techniques such as near-infrared (NIR) and Raman spectroscopy analyze the absorption or scattering of light at specific wavelengths, enabling in-situ, non-invasive testing [23]. In agricultural applications, for example, researchers can directly scan the surface of fruits and vegetables using Raman spectroscopy, completing residue analysis in seconds—without the need for grinding samples or solvent extraction, as required by traditional methods. This non-destructive nature is especially valuable for delicate produce like strawberries and grapes, preserving sample integrity while maintaining high testing efficiency and minimizing waste [24].

(2) High detection efficiency: Spectroscopic methods offer remarkable speed. While traditional chromatographic analysis may take 30 minutes to several hours per sample, fluorescence and surface-enhanced Raman spectroscopy (SERS) can deliver results in seconds. When integrated with automated systems, spectroscopic platforms can process hundreds of samples per hour [25]. Portable NIR spectrometers, for instance, are now widely used in field monitoring, enabling farmers to accurately assess pesticide degradation and avoid residue violations due to insufficient pre-harvest intervals [26]. This high-throughput capability significantly enhances the coverage and timeliness of food safety oversight.

(3) Simultaneous multi-residue detection: Spectroscopy excels in detecting multiple pesticide residues at once—a crucial advantage given the widespread use of pesticide mixtures. Traditional single-analyte methods are increasingly inadequate. In contrast, full-spectrum scanning combined with chemometric modeling allows spectroscopic techniques to identify multiple residues

simultaneously. Fourier-transform infrared (FTIR) spectroscopy, for example, coupled with principal component analysis (PCA), can clearly distinguish characteristic peaks of different pesticide classes—such as organophosphates and pyrethroids—providing an efficient solution for complex residue analysis [27]. This capability is particularly valuable in responding to sudden contamination incidents.

(4) Smart integration and cost-effectiveness: Modern spectroscopic technologies have made breakthroughs in integration and affordability [28]. By incorporating miniaturized optical components and AI algorithms, next-generation devices have significantly lowered operational barriers [29]. For example, smartphone-coupled, cloud-based Raman spectrometers allow field personnel to perform tests with minimal training. Moreover, spectroscopy eliminates the need for consumables such as chromatographic columns and high-purity solvents, reducing long-term operating costs to just 20–33% of traditional methods. This economic advantage makes spectroscopic technologies particularly suitable for resource-limited rural areas and small-to-medium enterprises.

Given the growing importance and promising potential of spectroscopic analysis in pesticide residue detection, this review provides a systematic overview of various spectroscopic techniques—their principles, methodologies, strengths, and limitations. It focuses on five key technologies: SERS, infrared spectroscopy, fluorescence spectroscopy, ultraviolet-visible (UV-Vis) spectroscopy, and HSI. The review examines their fundamental principles, application characteristics, suitable scenarios, and current technical constraints, while also outlining future development trends. The aim is to offer technical guidance and theoretical insights to support the optimization and broader adoption of spectroscopic detection in food safety and agricultural monitoring.

## 2. Principles and Applications of Spectroscopic Techniques

### *2.1. SERS Techniques*

Raman spectroscopy is a powerful tool for analyzing molecular structures, based on the detection of inelastic scattering that occurs when photons interact with molecules [30]. In 1928, C.V. Raman discovered that when laser light passes through a sample, in addition to elastic scattering (Rayleigh scattering), approximately 0.1% of the photons undergo a frequency shift—known as the Raman shift—generating two characteristic spectral lines: Stokes lines (with reduced frequency) and anti-Stokes lines (with increased frequency). This "molecular fingerprint" arises from vibrational energy level differences in chemical bonds, giving Raman spectroscopy a unique advantage in substance identification. For example, Dias et al. successfully constructed a comprehensive spectral database containing characteristic Raman profiles of 78 different pesticides in both liquid and solid forms. Their work provides a valuable technical reference for rapid pesticide detection. The database systematically annotates the characteristic Raman bands of each pesticide and organizes them by mode of action, chemical structure, active ingredient, and relative peak intensity, offering standardized data support for subsequent pesticide identification research. This achievement not only fills a critical gap in the application of Raman spectroscopy to pesticide analysis but also promotes collaborative innovation in the scientific community through its open-access, shared database model [31].

However, conventional Raman spectroscopy suffers from inherently weak signal intensity—typically only about $10^{-6}$ of the Rayleigh scattering signal. To overcome this limitation, significant technological advancements have been made to enhance detection capability. For instance, Fourier-transform Raman (FT-Raman) spectroscopy employs a 1064 nm NIR laser to effectively suppress fluorescence interference from samples. However, FT-Raman is susceptible to sample movement and prone to thermal drift, which can affect measurement stability [32]. In contrast, SERS has emerged as a major research focus by leveraging localized electromagnetic field effects generated by nanostructured substrates, enhancing detection sensitivity to the single-molecule level [33].

### 2.1.1. Principles

SERS has overcome the sensitivity limitations of traditional Raman spectroscopy, laying the foundation for trace detection [34,35]. SERS achieves significant enhancement of Raman signals through interactions between metal nanostructures and target molecules, involving both physical and chemical enhancement mechanisms [36,37]. The physical enhancement arises from localized surface plasmon resonance (LSPR) excited on the surfaces of metal nanoparticles (such as silver and gold). When illuminated by laser light, electromagnetic "hot spots" form on the metal surfaces, boosting the Raman scattering intensity of adsorbed molecules by factors of $10^6$ to $10^{14}$. Chemical enhancement relies on charge transfer between the metal substrate and the molecules, forming metal-molecule complexes that alter molecular polarizability, thereby enhancing the Raman signal by approximately $10^2$ times [38–40]. For example, Guo et al. demonstrated an enhancement factor of $1.39 \times 10^9$ using silver/graphene composite substrates optimized for nanoparticle size (around 60 nm) and distribution density, with acetone solvent promoting charge transfer between pesticide molecules and the substrate. Typical chemical enhancement factors range from $10^1$ to $10^3$, but they are sensitive to molecular orientation. When both mechanisms work synergistically (e.g., molecules adsorbed in hotspots of Au@Ag core-shell structures), the enhancement factor can reach $10^{10}$ to $10^{14}$, enabling single-molecule detection. Transition metal oxides (such as $TiO_2$) can also produce significant chemical enhancement through interface charge transfer involving defect energy levels [41].

In the detection of pesticide molecules, SERS demonstrates unique advantages [42,43]. By leveraging specific adsorption interactions between metal nanosubstrates and pesticide molecules, along with probe molecules (such as paraquat) to create a "bridging" model, SERS can capture weakly Raman-active organochlorine pesticides and excite identifiable signals [44]. In practical applications, flower-like silver nanoparticles substrates maintain pesticide structural integrity within a pH range of 6.66 to 11.11. Combined with droplet concentration methods, detection limits can be reduced to sub-ppb levels (e.g., 0.1 ppb), meeting the requirements for detecting trace residues in complex matrices like tea [15,45]. Compared to chromatographic methods, SERS requires no complex sample preparation, with each test taking only a few seconds, and it can distinguish isomers via characteristic peak shifts. As a non-destructive detection technique, SERS not only meets increasingly stringent food safety standards (such as the EU limit of 0.01 mg/kg) but also provides an efficient and portable tool for monitoring the quality and safety of agricultural products.

### 2.1.2. SERS Substrates and Signal Enhancement Strategies

The performance of SERS technology hinges on the rational design and optimization of substrate materials. Based on different enhancement mechanisms and material properties, the current mainstream SERS substrates can be categorized into three main types:

Precious metal substrates, including gold and silver nanostructures (such as nanospheres, nanorods, nanocubes, etc.), which offer enhancement factors ranging from $10^6$ to $10^8$. However, these materials are prone to oxidation and are relatively expensive [46,47].

Semiconductor substrates (such as $TiO_2$, $MoO_3$-x), which achieve charge transfer enhancement through defect engineering to control oxygen vacancies. Although their enhancement factors are lower ($10^2$ to $10^4$), they exhibit excellent chemical stability [48,49].

Composite functional substrates, including core-shell structures (such as $Au@SiO_2$), flexible substrates (such as PE film loaded with nanoparticles), and magnetic composite microspheres (such as $Fe_3O_4@Au$) [50,51].

Research indicates that the performance of SERS substrates is primarily influenced by three key factors: surface morphology, size parameters, and structural design. In terms of morphology, spherical nanoparticles exhibit uniform LSPR intensity, while polyhedral structures such as rods and cubes show angle-dependent enhancement effects [52]. Size effects demonstrate that when the size of silver nanoparticles increases from 50 nm to 100 nm, electromagnetic field coupling significantly enhances, leading to increased SERS signal intensity. Regarding structural design, three-dimensional array substrates fabricated using nanoimprint lithography can achieve enhancement factors in the range of $10^7$ to $10^8$. The unique short-range island distribution feature of these substrates effectively increases hotspot density and signal uniformity [53].

In summary, optimizing the performance of SERS substrates requires a comprehensive consideration of three critical factors: morphology (uniform spheres vs. anisotropic polyhedra), size (optimal electromagnetic coupling at 50-100 nm), and structural design (high hotspot density in 3D arrays). These research findings provide important theoretical guidance and technical pathways for developing high-performance SERS substrates.

#### 2.1.3. Research Progress of SERS in Pesticide Detection

SERS has demonstrated broad application potential in the detection of pesticide residues. In the analysis of fruits, vegetables, and milk, high-sensitivity detection has been achieved using SERS substrates such as gold and silver nanomaterials [54–56]. By further integrating chemometric methods, researchers have enabled rapid and quantitative detection of various pesticides—for instance, thiabendazole (TBZ) in citrus [57], mixed pesticide residues in apple and orange juices [58], and acetamiprid, methamidophos, and 2,4-D in tea leaves [59,60].

In the context of staple grains, herbs, and oil-bearing crops, a range of advanced substrates—including Ag@ZnO nanoflowers (NFs), chitosan-modified filter paper, and flower-like silver nanoparticles—have been successfully applied to detect deltamethrin in wheat [61], chlorpyrifos [62], paraquat and thiram in herbal samples [63], and acephate in crude palm oil [64]. These studies consistently highlight the high sensitivity, unique "molecular fingerprint" specificity, and strong adaptability of SERS in complex matrices. Collectively, they underscore SERS as a powerful tool for on-site, rapid screening in food safety monitoring, paving the way for real-time quality control across the agricultural supply chain.

#### SERS Technology in Pesticide Residue Detection in Fruits and Vegetables

SERS has shown tremendous potential in detecting pesticide residues in fruits and vegetables. From citrus to other fruits, vegetable surfaces, fruit juices, and tea leaves, SERS technology offers robust support for on-site rapid detection of food safety issues due to its high sensitivity and unique "molecular fingerprint" characteristics [65,66].

For instance, in the detection of TBZ in citrus, Qin et al. utilized SERS based on gold nanorods (Au NRs) combined with chemometric methods to achieve highly sensitive detection of TBZ residues in citrus. The Au NRs (39 × 22 nm), synthesized via a seed-mediated approach, exhibited a longitudinal plasmon resonance peak at 640 nm and a Zeta potential of +19.8 mV, significantly enhancing the Raman signal. By employing Air-PLS baseline correction and derivative preprocessing to eliminate interference, and using genetic algorithm-partial least squares (GA-PLS) to select 144 key variables, the model demonstrated excellent performance ($Rp^2 = 0.9737$, RPD = 5.85). This method achieved a detection limit as low as 0.33 μg/mL, far below the Chinese standard (10 mg/kg), with recovery rates of 83.50–98.50% (RSD $< 5\%$) and no significant difference from HPLC results ($p > 0.05$). Without requiring complex sample preparation, this method can complete detection within 10 minutes and specifically distinguish coexisting pesticides such as chloropyrifos, providing an efficient and stable solution for pesticide residue detection [57].

Building on these technological advancements, Guo et al. innovatively employed double-layer 4-mercaptobenzoic acid (MBA)-modified gold-silver core-shell nanoparticles (Au MBA@Ag MBA NPs) as SERS substrates to achieve efficient dual-mode detection of acetamiprid and benzimidazole in fruits. Through optimized substrate design, the detection limits reached 0.05 mg/kg and 0.03 mg/kg, respectively. This technique demonstrated excellent anti-interference capabilities in actual samples such as apples and pears (recovery rates of 85%–110%). Compared to traditional methods, this detection protocol offers advantages such as ease of operation (<10 minutes), high sensitivity (enhancement factor > 10^6), and provides reliable technical support for rapid on-site screening of pesticide residues in fruits [67].

In the realm of pesticide detection on fruit surfaces, Guo et al. developed a flexible SERS sensor based on electrospinning and self-assembly of nanomaterials (PAN/$Cu_2O$@Ag/Au@Ag) for rapid in-situ detection of thiram fungicide on apple surfaces (Figure 1a). The material preparation involved synthesizing PAN/$Cu_2O$@Ag flexible substrates via electrospinning and self-assembling Au@Ag core-shell nanoparticles on their surfaces, combining both SERS enhancement and photocatalytic self-cleaning functions. Spectral data were analyzed using convolutional neural networks (CNN) and competitive adaptive reweighted sampling-PLS (CARS-PLS) algorithms, with the CNN model demonstrating superior performance, achieving a correlation coefficient of 0.9963 and a detection limit as low as 0.020 mg/L, below international standard limits. Actual sample detection recovery rates ranged from 88.32% to 111.80%, with the sensor reusable for more than five cycles. Combined with UV photocatalytic degradation, this approach achieved efficient self-cleaning. This technology integrates nanomaterial design with deep learning, providing a highly sensitive and reproducible solution for on-site pesticide residue detection in agricultural products [68].

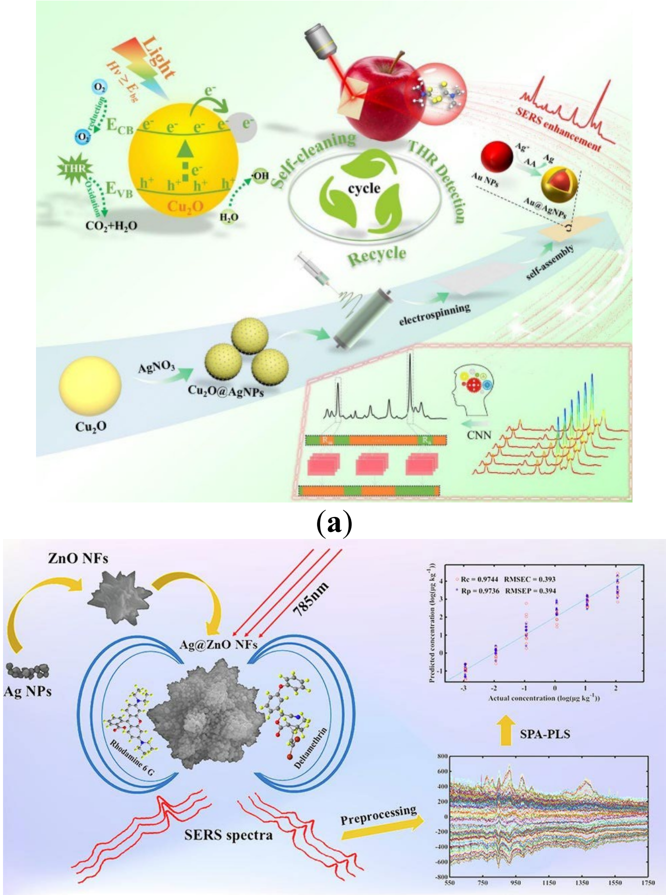

(a)

(b)

**Figure 1.** (**a**) PAN/Cu2O@Ag/Au@Ag flexible SERS sensor coupled with chemometrics for quantitative detection of thiram residues on apples [68] ; (**b**) Quantification of deltamethrin residues in wheat by Ag@ZnO NFs-based surface-enhanced Raman spectroscopy coupling chemometric models [61].

Notably, for pesticide residues on fruit and vegetable surfaces, Hong et al. innovatively simplified substrate preparation by using commercially available 3M 9080 tape as a flexible carrier. By optimizing gold nanoparticle (AuNPs) concentration (2.5-fold), dosage (80–120 μL), and sodium chloride coagulant ratio (10–15 μL), they constructed high-activity SERS substrates directly on the tape surface. This method successfully achieved ultra-trace detection of TBZ (20 ng/cm²), carbendazim (36 ng/cm²), and chlorpyrifos (80 ng/cm²) on tomato surfaces. Raman peak assignments were performed using density functional theory (DFT), and semi-quantitative models were established using least squares support vector machines (LSSVM) with an $R^2 \geq 0.864$, significantly enhancing detection accuracy. This strategy simplified the traditional "absorption-separation-dosing" process into a single "adhesion-detection" step. Portable Raman validation showed substrate stability up to 45 days, providing an efficient and practical solution for on-site screening of pesticide residues in agricultural products [69]. While these methods have significantly improved detection convenience and stability, there remains room for further optimization in sensitivity and controllability of hot spot structures. In this context, Li et al. developed a flexible SERS sensor based on electrospinning and electrostatic self-assembly (PDADMAC/PSS/Au@Ag NRs filter paper) for in-situ detection of non-systemic pesticides (methyl parathion, thiram, chlorpyrifos) on fruits and vegetables. CTAB-guided synthesis of Au@Ag core-shell nanorods was combined with PDADMAC (+) and PSS (-) modification of filter paper to achieve electrostatic self-assembly, forming three-dimensional SERS hotspots. Using 785 nm laser Raman spectroscopy and a "paste-read" method, direct acquisition of epidermal pesticide signals was achieved without complex preprocessing. Detection performance showed limits of detection (LODs) for methyl parathion, thiram, and chlorpyrifos as low as 0.072, 0.052, and 0.059 ng/cm², respectively, with a linear range of 0.051 ng/cm² to 5.096 μg/cm² ($R^2 > 0.988$). Actual sample recovery rates were between 64.68% and 126.80%. This sensor offers high sensitivity (LOD for 4-MBA at $10^{-12}$ M) and stability (RSD < 9.29%), providing a fast (<10 minutes), non-destructive solution for on-site pesticide residue detection on agricultural products [70].

For rapid and sensitive detection of pesticide residues in complex food matrices like juice, Lin et al. developed an SERS substrate based on vertically aligned gold nanorod arrays (AuNRs) for detecting carbamate insecticide carbaryl in juices and milk. Materials were synthesized via seed-mediated growth of AuNRs (length: 87.8 ± 8.9 nm, width: 27 ± 4.6 nm) and self-assembled on gold-coated silicon wafers to form vertical arrays, utilizing 785 nm laser excitation to enhance electromagnetic fields. During detection, samples were centrifuged and directly applied to the substrate without complex preprocessing. Results showed LODs for carbaryl in orange juice, grapefruit juice, and milk at 509, 617, and 391 ppb, respectively, all below US EPA maximum residue limits (juice: 10 ppm, milk: 1 ppm). Prediction models built using PLS showed correlation coefficients (r) between predicted and actual concentrations ranging from 0.88 to 0.95, with recoveries of 82%–97.5%. This method offers high sensitivity (minimum detectable level: 50 ppb), speed (sample preparation ~10 minutes), and good resistance to matrix interference, making it suitable for pesticide residue detection in complex food systems [71].

Building on this, Zou et al. developed an SERS substrate based on gold core-silver shell nanorods (Au@Ag NRs) for rapid detection of the fungicide TBZ (TBZ) in juices. Materials were synthesized via seed-mediated growth of AuNRs and silver shell deposition to form core-shell structures, with plasmonic resonance optimized by adjusting $AgNO_3$ volume (30–250 μL). Uniform nanorods (length: 87.8 ± 8.9 nm, width: 27 ± 4.6 nm) with a silver shell thickness of about 3 nm were obtained. Using 785 nm laser excitation, LODs for TBZ in apple juice and peach juice reached 0.032 ppm and 0.034 ppm, respectively, below EPA limits. Recoveries were 95–101%, with RSD ≤ 4.43%. This method leverages Au@Ag bimetallic synergistic effects (enhancement factor > $10^6$) and vertical adsorption of TBZ molecules' C-S bonds to the silver shell, significantly enhancing sensitivity. With only 30 minutes of preprocessing, it is suitable for rapid detection in complex food matrices [72].

To further expand the application of SERS technology in multi-residue detection, Cai et al. utilized portable Raman spectrometers and Au@Ag core-shell nanoparticles SERS substrates to simultaneously detect mixed pesticides (imidacloprid and thiram) in apple juice. By optimizing $AgNO_3$ dosage (500 μL/10 mL AuNPs), Au@Ag NPs with optimal SERS activity (~58.6 nm diameter) were obtained. Using 785 nm laser excitation, characteristic peaks at 635 cm⁻¹ (imidacloprid C–C–C vibration) and 1385 cm⁻¹ (thiram C–N vibration) were selected to build quantitative models. In apple juice matrix, LODs for imidacloprid and thiram were 1.22 μM (0.272 mg/L) and 0.076 μM (0.018 mg/L), respectively, both below EPA maximum residue limits (1 mg/L and 5 mg/L). Recovery rates were 90.2%–122.12% and 90.38%–113.42%. This method utilizes competitive adsorption mechanisms to distinguish target signals, with the entire detection process taking less than 10 minutes, significantly improving detection efficiency. It provides an efficient and practical technological pathway for rapid on-site analysis of multiple pesticide residues in agricultural products [58].

Additionally, researchers have extended SERS technology to tea, an important agricultural product, where the complex components, particularly polyphenols, pose significant challenges for detection selectivity and anti-interference performance. To address these challenges, research teams have developed two differentiated detection strategies tailored to tea samples, offering comprehensive solutions for monitoring agricultural product safety.

Chen et al. developed two distinct methods for pesticide detection in tea using SERS technology. Method (i) involves synthesizing 30 nm gold nanoparticles (GNPs) via sodium citrate reduction, adsorbing crystal violet (CV) as a reporter molecule, and introducing a specific aptamer (ACA) for the insecticide acetamiprid (AC) to achieve targeted recognition. When ACA binds with AC, it induces GNP aggregation in salt solutions, forming SERS "hot spots," thereby enhancing CV's characteristic peak signal at 1175 $cm^{-1}$. This method exhibits excellent detection performance with a linear range of $3.0 \times 10^{-8}$ to $4.0 \times 10^{-6}$ M and a detection limit as low as $1.76 \times 10^{-8}$ M. Recovery rates in green tea samples were 98.45%–104.5%, with relative standard deviations (RSD) less than 5% [59]. Method (ii) optimizes temperature conditions (25°C) to synthesize flower-like silver nanoparticles (AgNPs) with rough surfaces, achieving an enhancement factor of $1.39 \times 10^6$ as SERS substrates. Combining solid-phase extraction (SPE) preprocessing techniques, methamidophos, acetamiprid, and 2,4-D were extracted from tea using 80% acetonitrile-water solution, effectively removing matrix interference. SERS detection results showed linear ranges of $1.0 \times 10^{-3}$–$10^3$ μg/mL for methamidophos and acetamiprid, and $1.0 \times 10^{-2}$–$10^3$ μg/mL for 2,4-D, with LODs of $5.58 \times 10^{-4}$, $1.88 \times 10^{-4}$, and $4.72 \times 10^{-3}$ μg/mL, respectively, all below EU maximum residue limits. Recovery rates were 84.51%–92.58%, with RSD less than 5%, indicating high sensitivity and accuracy. Both methods utilize electromagnetic enhancement mechanisms to identify pesticide characteristic peaks, providing highly sensitive and selective solutions for pesticide residue detection in tea. Method (i) achieves specific recognition through aptamer conformation changes, while method (ii) enhances signals through the rough surface of AgNPs, each offering unique advantages that can be flexibly chosen based on actual detection needs. These studies provide new technological pathways for rapid and accurate detection of pesticide residues in complex matrices such as tea [60].

### Pesticide Detection in Grains and Oil Crops

SERS has broad applications in grains and oil crops, a crucial agricultural sector characterized by complex matrix components and diverse pesticide residues, posing new challenges for detection technologies. Researchers have carefully designed various SERS detection schemes tailored to the specific characteristics of different crops.

Addressing the issue of deltamethrin residue in wheat, Chen et al. developed a novel SERS detection method based on silver nanoparticle-modified zinc oxide nanoflowers (Ag@ZnO NFs) for the rapid quantitative analysis of deltamethrin residues in wheat (Figure 1b). The Ag@ZnO NFs, synthesized via wet chemistry methods, feature a three-dimensional structure with an enhancement factor reaching $10^7$, effectively boosting the Raman signal of target molecules. After ethanol extraction of samples, mean centering (MC) preprocessing and successive projections algorithm-PLS regression (SPA-PLS) modeling were employed, achieving a detection limit of 0.16 μg/kg, with a linear range of $1.0 \times 10^{-3}$ to $10^2$ μg/kg. The spiked recovery rates ranged from 96.33% to 109.17% (RSD < 5%). By optimizing substrate morphology and chemometric models, this method significantly enhanced detection sensitivity and accuracy, providing an efficient solution for monitoring pesticide residues in agricultural products [61].

Notably, researchers have developed differentiated detection strategies for various types of pesticide residues in wheat. For instance, to detect chlorpyrifos, an organophosphate pesticide, Huang et al. utilized more affinity-based substrate materials combined with SERS to achieve highly sensitive detection of its residues in wheat. Using wet chemistry synthesis of Ag@ZnO nanoflowers (Ag@ZnO NFs), their three-dimensional structure and LSPR effects reduced the detection limit of deltamethrin to 0.16 $\mu g \cdot kg^{-1}$, with recovery rates ranging from 96.33% to 109.17%. The use of mean centering-SPA-PLS (MC-SPA-PLS) models optimized prediction performance (Rp = 0.9736). Another study used chitosan-modified filter paper (Ch/AgNPs/paper) as a substrate, optimizing acetic acid concentration (1.5% optimal) to enhance the uniform distribution of silver nanoparticles, achieving a chlorpyrifos detection limit of 0.000558 $mg \cdot L^{-1}$. Normalized PLS model prediction correlation coefficients reached 0.9764, with recovery rates of 97.25%–119.38% [62].

Shifting focus from solid grain crops to liquid oil detection, SERS technology demonstrates remarkable adaptability and detection capabilities. In the highly complex matrix of crude palm oil, SERS technology excels particularly well. Addressing acephate (ACE) residue issues in crude palm oil, Li et al. employed flower-like silver nanoparticles (AgNPs) as substrates, combined with the random frog (RF) algorithm, to achieve high-sensitivity precise detection. This method achieved a detection limit as low as 4.69 ng/g, exhibited excellent linearity ($R^2 > 0.99$), and demonstrated high recovery rates (93.89%–108.32%), fully demonstrating the robust capability of SERS technology in liquid oil detection [64].

### Application of Chemometrics Combined with SERS Technology in Pesticide Detection

Data processing in SERS has evolved into an innovative, multi-technology analytical framework. In the field of chemometrics, PCA enables efficient data compression through feature space reconstruction, PLS establishes precise quantitative relationships between spectral signals and analyte concentrations, while the Random Frog (RF) algorithm significantly enhances model generalization by intelligently selecting key spectral variables [73,74]]. Complementing these traditional methods are emerging deep learning techniques: CNNs can automatically extract complex spectral features, and transfer learning effectively addresses the challenge of limited training data in real-world applications [75].The synergistic application of these approaches—such as combining PCA-based preprocessing with deep learning models—leverages the interpretability of chemometric methods while fully exploiting the nonlinear modeling power of intelligent algorithms. This hybrid strategy enhances both accuracy and robustness in SERS-based detection, particularly in complex matrices.

This synergistic effect is particularly evident in the detection of pesticide residues in tea. Chen et al. developed an innovative analytical platform that integrates SERS with chemometric modeling for the detection of chlorpyrifos residues in tea. The team designed and synthesized core-shell Au@Ag nanoparticles as SERS substrates, which exhibited a high enhancement factor of $2.5 \times 10^6$. For qualitative analysis, a K-Nearest Neighbors (KNN) algorithm combined with second-derivative spectral preprocessing achieved highly accurate classification of chlorpyrifos-contaminated tea samples, with classification accuracy ranging from 90.84% to 100%. In quantitative analysis, genetic algorithm-optimized models—GA-PLS and siPLS-GA—were applied to Standard Normal Variate (SNV)-preprocessed spectra, yielding excellent predictive performance: determination coefficients ($r^2$) reached 0.96–0.98, and root mean square errors (RMSE) of prediction (RMSEP) were maintained between 0.29 and 0.31. No statistically significant difference was observed between the results of this method and reference GC-MS measurements ($p > 0.05$), and the detection limit was as low as $3.0 \times 10^{-9}$ mol/L. This integrated approach provides a rapid and highly sensitive tool for quality control and safety monitoring in the tea industry [76].

Notably, Chen et al. further advanced this methodology by combining octahedral hollow Au-Ag cages (Au-Ag OHCs) with a CNN algorithm. The unique plasmonic structure of the Au-Ag OHCs provided strong electromagnetic enhancement, while the CNN enabled intelligent feature extraction from complex spectral data, pushing detection sensitivity into the parts-per-billion (ppb) range. By synergistically applying CNN, PLS, and Extreme Learning Machine (ELM) algorithms, the method achieved accurate quantitative prediction of thiram and pymetrozine residues in tea. Statistical comparison with HPLC reference data revealed no significant difference ($p > 0.05$), confirming the reliability and accuracy of the SERS-chemometrics framework [77].

## Application of Molecularly Imprinted Polymers (MIPs) with SERS Technology in Pes-ticide Detection

SERS is highly sensitive but can be susceptible to interference from coexisting substances in complex matrices, limiting its practical applications. To address this issue, researchers have combined MIPs, which possess specific recognition capabilities, with SERS technology. This integration has led to the development of novel sensing platforms that offer both high sensitivity and selectivity, providing robust support for rapid and accurate detection of pesticide residues in food [78,79].

MIPs are typically synthesized using target pesticides or their structural analogs as template molecules. These templates interact with functional monomers (e.g., methacrylic acid, acrylamide) and cross-linkers (e.g., ethylene glycol dimethacrylate) to form specific recognition cavities. The resulting MIPs are then integrated with SERS substrates such as gold/silver nanoparticles or magnetic $Fe_3O_4@SiO_2$ composite materials (Figure 2a), forming either "one-step" or "two-step" sensors [80].

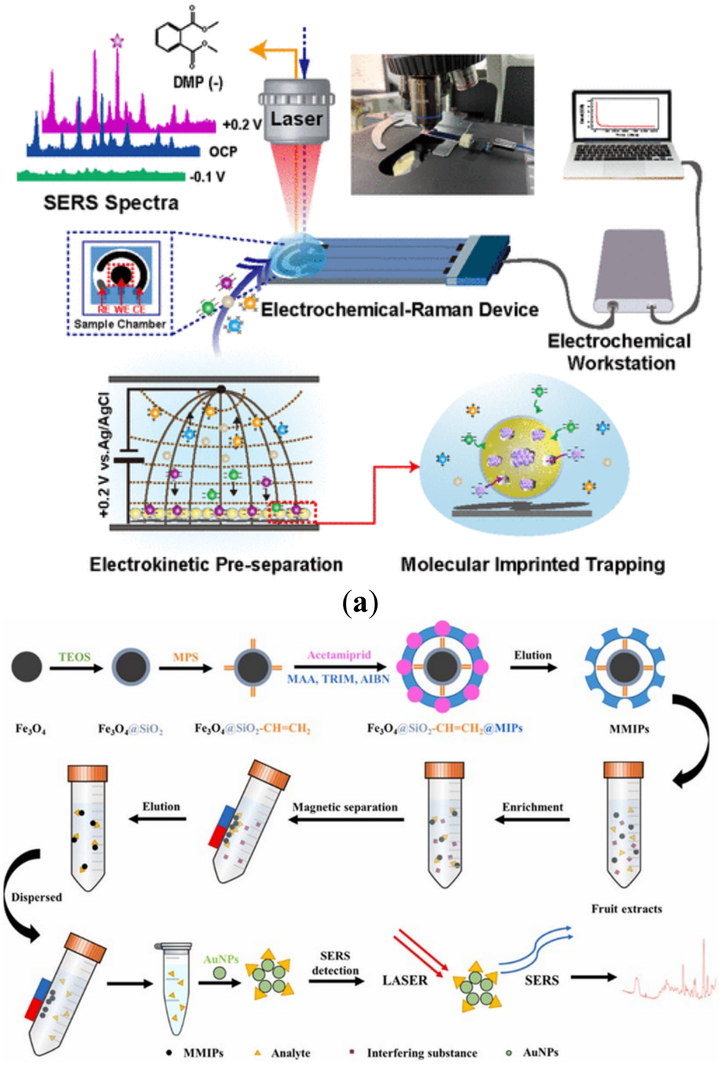

(a)

(b)

**Figure 2.** (**a**) Illustration of Electrokinetic Preseparation and Molecularly Imprinted Trapping of Charged PAEs on a Portable Interface for Selective SERS Recognition [80]; (**b**) Detection of neonicotinoids in agricultural products using magnetic MIPs-surface enhanced Raman spectroscopy [81].

For the detection of lipophilic pesticides, traditional aqueous-phase SERS systems are not suitable. Neng et al. developed MIPs using methyl methacrylate (MMA) as the functional monomer and pentachloronitrobenzene (PCNB) as the template molecule, integrating oil-soluble silver nanoparticles as the SERS-active substrate. The prepared MIPs exhibited specific recognition capability towards PCNB, with an adsorption equilibrium time of only 120 minutes. Using the optimized SERS-MIPs method, a good linear relationship was observed within the concentration range of 0.005–0.15 μg/mL, with a detection limit of 5.0 ng/mL. In spiked rice samples, recovery rates were between 94.4% and 103.3%, with RSD ranging from 4.6% to 7.4%, consistent with GC-MS results. This method combines the selective enrichment capability of MIPs with the high sensitivity of SERS, offering a rapid and reliable solution for detecting lipophilic pesticide residues in food matrices [82].

In the context of detecting hydrophilic and polar pesticides, researchers have further enhanced the performance of SERS-MIPs sensors by optimizing functional monomers and substrate structures. Yan et al. developed MIPs integrated with gold nanoparticles (AuNPs), combined with SERS technology for simultaneous detection of triazine herbicides prometryn and simetryn. Through precipitation polymerization, MIPs with specific-like recognition properties were synthesized, exhibiting imprinting factors of 5.3 and 4.2 (at an initial concentration of 10 μg/mL) for prometryn and simetryn, respectively, with an adsorption equilibrium time of only 60 minutes. Optimized AuNPs (~50 nm diameter) served as the SERS substrate, with NaCl used as an aggregating agent. Quantitative methods were established at characteristic peaks of 974 $cm^{-1}$ (prometryn) and 1074 $cm^{-1}$ (simetryn). The method demonstrated detection limits of 20 μg/kg in rice and wheat samples, with a linear range of 0.02–0.5 μg/mL. Recovery rates ranged from 72.7% to 90.9% (RSD: 1.7%–7.8%), and effective elimination of matrix interference in grain samples was achieved through the combination of MIPs with QuEChERS, enabling highly selective detection of dual residues in complex samples [83].

Cao et al. developed a novel detection method based on magnetic MIPs coupled with surface-enhanced Raman spectroscopy (MMIPs-SERS) (Figure 2b) for the rapid analysis of neonicotinoid pesticides (acetamiprid and thiacloprid) in agricultural products. By employing surface imprinting techniques to polymerize an imprinting layer on the surface of magnetic nanoparticles, they created core-shell structured MMIPs that achieve adsorption saturation within just one minute and exhibit specific-like recognition capabilities towards the target analytes. The optimized MMIPs-SERS system demonstrated a linear detection range of 1–20 μg/g for acetamiprid and thiacloprid in pear and peach samples, with detection limits of 23.7–68.8 ng/g and 23.7–36.4 ng/g, respectively. The spiked recovery rates ranged from 73.5% to 112.8%, with (RSD below 7.0%, validating the high sensitivity and accuracy of this method. This approach leverages the selective enrichment capability of MMIPs and the rapid analysis advantages of SERS, providing an efficient solution for detecting trace pesticide residues in complex matrices [81].

Xu et al. reported a highly sensitive SERS sensor based on magnetic MIPs (Mag@MIP NPs) combined with gold nanoparticles (Au NPs) for the detection of 2,4-dichlorophenoxyacetic acid (2,4-D) in food and water. Magnetic nanoparticles (200 nm diameter) were synthesized using $FeCl_3 \cdot 6H_2O$ and chitosan, and an imprinting layer was formed by polymerizing acrylamide functional monomers and ethylene glycol dimethacrylate (EGDMA) cross-linkers in the presence of 2,4-D template molecules, resulting in a 14 nm thick imprinting layer. The Mag@MIP NPs specifically captured 2,4-D via hydrogen bonding, achieving adsorption equilibrium within 120 minutes. Subsequently, the SERS signal was enhanced through electrostatic adsorption onto Au NPs, with characteristic peaks at 1071 $cm^{-1}$. The sensor exhibited a linear response in the concentration range of 0.1–$10^5$ ng/mL ($R^2$ = 0.988), with a detection limit as low as 0.00147 ng/mL. Spiked recovery rates for milk and tap water samples were between 93.5% and 102.2%, showing no significant difference compared to HPLC results ($p > 0.05$). This demonstrates the excellent selectivity and practicality of the sensor [84].

To further enhance sensor performance, some studies focus on the synergistic optimization of functional monomers and substrate morphology. For instance, Li et al. developed a self-cleaning R6G detection sensor using zinc oxide nanorods (ZnO NRs) as the substrate and silver nanoparticles (AgNPs)-modified ZnO/Ag heterostructures (ZOA) as the SERS-active substrate, combined with molecular imprinting technology. During the preparation process, acrylamide was used as the functional monomer and ethylene glycol dimethacrylate as the cross-linker to construct R6G-specific recognition cavities on the ZOA surface, achieving an imprinting factor of 5.3. The optimized ZOA-

Preprints.org (www.preprints.org) | NOT PEER-REVIEWED | Posted: 22 September 2025 doi:10.20944/preprints202509.1694.v1

MIPs exhibited excellent selectivity at the characteristic peak of 1654 $cm^{-1}$, with a detection limit of $10^{-13}$ mol/L ($R^2 = 0.996$) and an enhancement factor of $3.3 \times 10^5$. Cross-reactivity with structurally similar compounds such as rhodamine B and crystal violet was below 30%. Under UV light irradiation, the sensor could achieve self-cleaning through photocatalysis, maintaining over 92% signal stability after five cycles of use. This demonstrates high sensitivity, selectivity, and reproducibility [85].

Additionally, the "two-step" strategy offers new approaches for detecting pesticide residues in complex matrices. Hua et al. synthesized specific MIPs targeting 2,4-dichlorophenoxyacetic acid (2,4-D) and innovatively combined them with AgNPs-modified SERS substrates. Using molecularly imprinted solid-phase extraction (MISPE) technology, they selectively enriched 2,4-D from milk samples, establishing a highly sensitive detection method at the characteristic peak of 391 $cm^{-1}$. This method demonstrated excellent analytical performance: a detection limit as low as 0.006 ppm, a quantification limit of 0.008 ppm, and a good logarithmic linear relationship within the concentration range of 0.01–1 ppm ($R^2 = 0.9887$), fully covering the maximum residue limits set by European and American regulations for 2,4-D in milk (0.01–0.05 ppm). By optimizing the QuEChERS pretreatment combined with MISPE technology, the spiked recovery rates for milk samples were stable between 85% and 95%, with RSD below 8%. The entire detection process took only 20 minutes, providing a reliable technique for rapid screening of pesticide residues in dairy products [86].

The integration of SERS with MIPs has demonstrated significant potential in pesticide residue detection. By rationally designing functional monomers, optimizing substrate architectures, incorporating functionalities such as magnetic separation or self-cleaning, and employing "two-step" enrichment strategies, this hybrid approach has been successfully applied to the highly sensitive and selective detection of various pesticides—ranging from lipophilic and hydrophilic compounds to those present in complex matrices. Future research could focus on expanding the multi-residue recognition capability of MIPs, improving the stability and reproducibility of SERS substrates, and advancing the practical implementation of this technology in on-site, rapid screening for food safety monitoring.

In summary, these technological innovations have collectively driven a leap forward in SERS-based detection. Continuous advancements in substrate materials, coupled with algorithmic optimization, have enabled SERS to overcome the longstanding challenges of detecting trace-level pesticides in complex food matrices. The technique's unique molecular fingerprinting capability ensures accurate target identification, while diversified substrate designs enable multiple pathways for signal enhancement. The synergistic use of chemometric and deep learning algorithms not only significantly improves detection accuracy but also establishes a complete technical pipeline—from measurement and analysis to data processing [87]. These breakthroughs offer rapid, non-destructive solutions for food safety monitoring and hold great promise for large-scale industrial applications.

### 2.1.4 Comparison of Various SERS Detection Methods

Table 1 provides a systematic comparison of multiple SERS (SERS) detection methods used in pesticide residue analysis, highlighting significant advancements in sensitivity, accuracy, and practicality. Overall, various SERS methods generally exhibit high detection sensitivity, with limits of detection (LOD) ranging from ppm to ppb levels, and even down to $ng/cm^2$ or ng/g. Some advanced strategies demonstrate exceptional trace detection capabilities; for instance, the LOD for 2,4-dichlorophenoxyacetic acid (2,4-D) reaches as low as 0.00147 ng/mL [84], while the integration of convolutional neural network (CNN) models achieves an LOD of thiram as low as 0.286 ppb [77]. These examples underscore the immense potential of combining SERS with intelligent algorithms for signal resolution and sensitivity enhancement.

In terms of detection accuracy, most methods achieve recovery rates within the ideal range of 80%–120%. For example, recovery rates for acetamiprid and cypermethrin are 93.86%–105.64% and 92.62%–102.3%, respectively [67], indicating good quantitative reliability. Additionally, RSD are generally low (mostly <10%). For instance, the RSD for thiram detection is 2.29% [54], demonstrating excellent repeatability and stability of the results.

The widespread use of portable Raman spectrometers has significantly reduced detection times to within 5–30 minutes, greatly enhancing the feasibility of on-site rapid screening [54,56,72,81]. Further improvements in detection performance have been achieved by incorporating chemometrics, MIPs, or core-shell nanomaterials. For example, MIPs-SERS achieves an LOD of 0.005 μg/mL for pentachloronitrobenzene (PCNB) with stable recovery rates of 94.4%–103.3% [82], while SERS combined with chemometrics achieves an LOD of 0.16 $\mu g \cdot kg^{-1}$ for deltamethrin [61]. Although confocal Raman microscopy may extend detection times (e.g., up to 2 hours) [84], it enables ultra-trace analysis with extremely high precision.

In summary, SERS technology demonstrates powerful application potential in pesticide residue detection due to its high sensitivity, rapid response, and good reproducibility. When integrated with new materials, advanced algorithms, and portable devices, SERS approaches increasingly meet the comprehensive needs of efficient, precise, and on-site detection in real-world scenarios. This combination not only enhances target selectivity but also significantly improves overall detection performance, making it an invaluable tool for food safety monitoring.

doi:10.20944/preprints202509.1694.v1

**Table 1.** Detection performance comparison of various detection methods.

| Detection Scheme | Data Analysis Methods | Pesticides | Recovery Rate (%) | RSD (%) | LOD | Detection Time | Reference |
|---|---|---|---|---|---|---|---|
| SERS | Portable Raman spectrometer (785 nm) | Thiram | -- | 2.29 | 1 ppm | 5–10 min | [54] |
| SERS | Portable Raman spectrometer | Melamine; Thiram | Melamine in milk: 95.9；Thiram in apple juice: 94.8 | Melamine:3.53；Thiram: 4.49 | Melamine: 7.38 μg/L；Thiram: 86.1 μg/L | <10 min | [56] |
| SERS with stoichiometry | - | TBZ | Good recycling performance | < 10 | 0.1 mg/kg | <10 min | [57] |
| SERS | Portable Raman spectrometer | Acetamiprid; Thiram | Acetamiprid: 90.2–122.12 (apple juice), 89.86–117.23 (orange juice); Thiram: 90.38–113.42(apple juice), 91.46–108.72 (orange juice) | Acetamiprid, Thiram | Acetamiprid: 0.272 mg/L(apple juice), 0.47 mg/L(orange juice); Thiram: 0.018 mg/L(apple juice),0.025 mg/L(orange juice) | - | [58] |
| SERS with stoichiometry | SPA-PLS | Deltamethrin | 96.33–109.17 | < 5 | 0.16 μg·kg$^{-1}$ | - | [61] |
| SERS | Portable Raman spectrometer | Acetamiprid (ACE); Cypermethrin (CBZ) | ACE: 93.86–105.64；CBZ: 92.62–102.3 | - | ACE: 0.27 μg/kg；CBZ: 1.71 μg/kg | - | [67] |
| SERS with stoichiometry | - | Thiram | 88.32–111.80 | 2.92–4.91 | 0.020 mg/L | - | [68] |
| SERS | - | Methyl-parathion (MP); Thiram(TMTD), Chlorpyrifos (CPF) | MP: 81.77–118.67；TMTD: 64.68–117.20；CPF: 73.10–126.80 | 8.58 (1078 cm$^{-1}$), 9.29 (1583 cm$^{-1}$) | MP: 0.072 ng/cm$^{2}$；TMTD: 0.052 ng/cm$^{2}$；CPF: 0.059 ng/cm$^{2}$ | - | [70] |

| | | | | | | | |
|---|---|---|---|---|---|---|---|
| SERS | Confocal Laser Scanning Raman Microscope System (InVia Reflex, Renishaw, UK) | Carbaryl | 82–99.8 | - | - | - | [71] |
| SERS | Confocal Laser Scanning Raman Microscope System (Renishaw, UK) | Thiabendazole (TBZ) | 95–101 | - | TBZ: 0.032 ppm (Apple juice), 0.034 ppm (Peach juice) | <30 min | [72] |
| SERS with stoichiometry | | Pymetrozine; Thiram | - | <8% | 0.0001 μg/mL | - | [74] |
| SERS with stoichiometry | GC-MS | Chlorpyrifos (CPS） | - | - | - | - | [76] |
| SERS with Convolutional Neural Network (CNN) Model | | Thiram; Pymetrozine | Thiram: 83.06–92.6; Pymetrozine: 95.32–110.38 | Thiram:6.43; Pymetrozine:10.41% | Thiram:0.286 ppb; Pymetrozine:29 ppb | - | [77] |
| SERS with Molecular Imprinting Technology (MIPs) | - | Pentachloronitrobenzene (PCNB) | 94.4–103.3 | 4.6–7.4 | 0.005 μg/mL | - | [82] |
| SERS with MIPs | Portable Raman spectrometer (RT5000, 785 nm) | Simazine; Prometryn | Simazine: 72.7–90.9; Prometryn: 79.1–86.5 | Simazine:1.7–7.6; Prometryn: 2.3–7.8 | 0.05 μg·mL$^{-1}$ | - | [83] |
| SERS | SPLD-RAMAN spectrometer (785 nm) | 2,4-Dichlorophenoxyacetic acid (2,4-D) | 93.5–102.2 | - | 0.00147 ng/mL | 2 h | [84] |
| SERS | Portable Raman spectrometer (785 nm) | Acetamiprid; Thiacloprid | Acetamiprid: 85.1–107.6(pear), 86.1–98.2(Peach)；Thiacloprid: 90.1–105.6(pear),73.5– | 7.5 | Acetamiprid: 68.8 ng/g (pear), 33.7 ng/g (Peach); Thiacloprid: 36.4 ng/g (pear), 23.7 | - | [81] |

doi:10.20944/preprints202509.1694.v1

| | | | | | | | |
|---|---|---|---|---|---|---|---|
| | | | 112.8(Peach) | | ng/ | | |
| SERS | Portable Raman spectrometer (785 nm) | Thiram; Carbendazim; TBZ; Carbaryl | -- | 4.65 | $<10^{-15}$mol/L | - | [87] |

**Table 2.** Detection performance comparison of various detection methods based on Fluorescence spectrum.

| **Detection Scheme** | **Data Analysis Method** | **Pesticides** | **Recovery Rate (%)** | **RSD (%)** | **LOD** | **Detection Time** | **Reference** |
|---|---|---|---|---|---|---|---|
| Fluorescence spectrum with biosensor | Fluorescence imaging system | Paraoxon;<br>Dichlorvos;<br>Parathion;<br>Deltamethrin | 98.7–109.2 | 5.46–14.80 | $< 1.2 \times 10^{-12}$ M | <20 min | [105] |
| Fluorescence spectrum with biosensor | Fluorescence immunosensor | Fipronil | 95.95–137.07 | 0.07–0.23 | 0.01 μg/L | - | [110] |
| Fluorescence spectrum | Bionic fluorescence sensor | Phorate | 87.69–106.12 | < 11.16 | 0.0017μg/L | 45 s | [111] |
| Excitation-Emission Matrix Fluorescence Spectroscopy | Fluorescence spectrophotometer (250–600 nm) | Tsumacide (TSU);<br>Carbaryl (CBL) | TSU: 98.94;<br>CBL: 99.25 | - | TSU:0.147 ug/mL;<br>CBL:0.159 ug/mL | <dozens of minutes | [114] |
| NIR Fluorescence | NIR Fluorescent Prob（CES-targeted probe 1） | Isocarbophos;<br>Other typical OPs | 97.63–100.21 | 2.32–5.62 | 0.030 ug/L | Dozens of minutes | [115] |
| NIR Fluorescence | - | Dichlorvos;<br>Trichlorfon | Dichlorvos:96.50–01.83;<br>Trichlorfon:97.09–102.71 | - | Dichlorvos:18.9 ug/L;<br>Trichlorfon:16.529 ug/L | - | [116] |
| Dual-signal fluorescence spectrum | Glove sensor (365 nm) | Chlorpyrifos (CP) | - | ≤12 | $89 \times 10^{-9}$ M | 30 s | [120] |
| Turn-on fluorescence | - | Dichlorvos;<br>Trichlorfon;<br>Profenofos | 84.5–106.3 | 1.3–10.5 | Dichlorvos: 0.2 μg/L;<br>Trichlorfon: 5 μg/L:<br>Profenofo: 5 μg/L | Within a few minutes | [111] |
| Fluorescence | Fluorescence Spectrophotometer | Chlorpyrifos | 94.5–106.7 | < 11.51 | 0.015 ng/mL | 180 min | [125] |

| | | | | | | | |
|---|---|---|---|---|---|---|---|
| Spectroscopy | (425 nm) | | | | | | |
| Fluorescence Spectroscopy | - | Phorate | 87.69–106.12 | < 11.16 | 1.7 pg/L | 45 s | [129] |
| Fluorescence Spectroscopy | Dual-color excited fluorescent sensing technology (310 nm and 360 nm) | Atrazine;<br>Carbaryl;<br>Chlorpyrifos;<br>Prometryn | Atrazine: 96.0– 104.0;<br>Carbaryl: 95.5–103.5;<br>Chlorpyrifos: 997.0–105.0;<br>Prometryn: 96.5– 104.5 | Atrazine: 1.8–3.2;<br>Carbaryl: 2.1–3.5;<br>Chlorpyrifos: 1.6–3.0;<br>Prometryn: 1.9– 3.3 | Atrazine: 0.091 μM;<br>Carbaryl: 0.103 μM;<br>Chlorpyrifos: 0.087 μM;<br>Prometryn: 0.095 μM | <5 min | [131] |
| Fluorescence spectrum with Smartphone Image Recognition | - | Carbaryl | 97.85–103.10 | 0.64–1.44 | $27.40\times 10^{-9}$ M | Dozens of minutes | [133] |
| Fluorescence spectrum with Partial Least Squares (PLS) model | LS55 Fluorescence Spectrometer（Perkin Elmer） | - | - | - | 0–0.0305 mg/mL | Suitable for online onitoring | [134] |
| Multicolor fluorescence signal | - | Chlorothalonil (CTN);<br>Paclobutrazol (PBZ);<br>Fipronil（FIP） | - | - | CTN: 0.038 ng/mL;<br>PBZ: 0.025 ng/mL;<br>FIP: 0.046 ng/mL | <5 s | [135] |

doi:10.20944/preprints202509.1694.v1

## *2.2. Infrared Spectroscopy*

### 2.1.2. Principles

The core of infrared (IR) spectroscopy lies in the interaction between molecular vibrational energy levels and infrared radiation. When the frequency of incident light matches the vibrational frequency of a molecule's chemical bonds, the molecule absorbs specific wavelengths of energy through changes in its dipole moment, resulting in characteristic absorption bands [88]. This technique can be divided into three spectral regions based on wavelength: the near-infrared region (0.75–2.5 μm), which mainly reflects overtones of molecular vibrations; the mid-infrared region (2.5–25 μm), which contains rich information about fundamental vibrational modes; and the far-infrared region (25–1000 μm), which involves changes in molecular rotational energy levels [89]. Current research indicates that mid-infrared spectroscopy, due to its higher resolution and specificity, has become the primary method for structural analysis of substances [90]. However, when applying IR spectroscopy to trace analytes, it is limited by low infrared absorption cross-sections. Surface-enhanced infrared absorption spectroscopy (SEIRAS), an advanced form of IR spectroscopy, overcomes this limitation [91].

In the field of pesticide residue detection, infrared spectroscopy exhibits unique advantages. NIR spectroscopy, with its rapid detection capabilities, is suitable for preliminary screening of active ingredients such as deltamethrin in pesticide formulations. However, its analysis results are constrained by interference from water and model stability issues [92]. In contrast, mid-infrared spectroscopy can establish more precise quantitative models by leveraging characteristic absorptions of functional groups like C=O and C-N in pesticides such as imidacloprid, combined with PLS regression algorithms. Additionally, SEIRAS technology can overcome the limitations of sensitivity and precision inherent in conventional mid-infrared spectroscopy [93].

### 2.2.2. Research Progress of Infrared Spectroscopy in Pesticide Detection

With the rapid development of infrared spectroscopy technology, its application in the detection of dithiocarbamate (DMD) pesticides has gradually gained attention. Alessandra et al. developed a method based on flow injection-Fourier transform infrared spectroscopy (FI-FTIR) for the determination of ziram and thiram in solid samples. This study involved loading silver nanoparticles (10–100 nm in diameter) onto a copper foam substrate via a displacement reaction method. The process was optimized with parameters such as silver nitrate concentration (0.2 mmol/L), polyvinylpyrrolidone (PVP) amount (2 mL), and reaction time (30 seconds) to successfully prepare a transmission surface-enhanced infrared absorption spectroscopy (T-SEIRAS) active substrate. Scanning electron microscopy (SEM) and X-ray photoelectron spectroscopy (XPS) characterization confirmed that the silver nanoparticles were uniformly distributed on the substrate surface. This substrate achieved a 32.7-fold enhancement in the infrared absorption signal of the probe molecule MUA at 1689 $cm^{-1}$ and a 2.9-fold enhancement for thiram at 1371 $cm^{-1}$. By constructing a linear response model for thiram at 1236 $cm^{-1}$ ($R^2 = 0.923$), the detection limit reached as low as 0.024 mg/mL. This method offers advantages such as fast detection (approximately 5 minutes) and low cost, providing new insights for on-site rapid pesticide residue detection [94].

Notably, breakthroughs in SEIRA technology not only offer new methods for detecting specific pesticides like thiram but also enhance overall detection capabilities through innovations in substrate materials. This material-driven technological advancement is driving pesticide residue detection toward higher sensitivity and broader applicability.

The latest breakthroughs in SEIRA technology for pesticide residue detection are mainly reflected in three aspects: （1）Innovations in Substrate Materials: Researchers have developed novel noble metal nanostructures (such as gold and silver nanoparticles) and cutting-edge nanomaterials like graphene and hybrid perovskites, creating high-performance SEIRA substrates. These material innovations have significantly improved infrared signal sensitivity by up to three orders of magnitude, with enhancement factors reaching $10^3$-$10^4$ [95]. （2）Optimization of Detection Methods: Improvements in spectral acquisition parameters and signal processing algorithms have further enhanced detection accuracy and stability. （3）Expansion of Application Scenarios: The technology has been successfully applied to new areas such as complex matrix detection and on-site rapid screening. This triad of material innovation, method optimization, and expanded applications is driving pesticide residue detection technology toward higher sensitivity and stronger interference resistance.

### High-Performance SEIRA Enabled by Metallic Nanostructures

Pereira et al. developed a green analytical method for detecting atrazine (ATZ) by combining surface-enhanced infrared absorption spectroscopy (SEIRA) with silver selenide quantum dots ($Ag_2Se$/MPA) (Figure 3). The $Ag_2Se$/MPA quantum dots (6 ± 3 nm in size) were synthesized via a one-pot method and used as the SEIRA-active substrate. Coupled with attenuated total reflection infrared spectroscopy (ATR-IR), the method leverages electrostatic interactions and electromagnetic enhancement between the quantum dots and ATZ molecules to achieve an 86-fold signal enhancement at 1547 $cm^{-1}$ (νC═N stretching vibration). The method demonstrated a low detection limit of 0.001 μg/mL (1 ng/mL) and a linear range of 0.1–50 μg/mL. Validation using a PLS regression (PLSR) model showed recovery rates consistent with those obtained by chromatographic methods, while eliminating the need for the complex sample preparation typically required in conventional chromatography. This SEIRA-based strategy significantly enhances the sensitivity of infrared detection, meeting the regulatory limits for ATZ in water set by Brazil and the European Union (2 μg/L). It offers a rapid, cost-effective, and environmentally friendly solution for monitoring environmental pollutants [96].

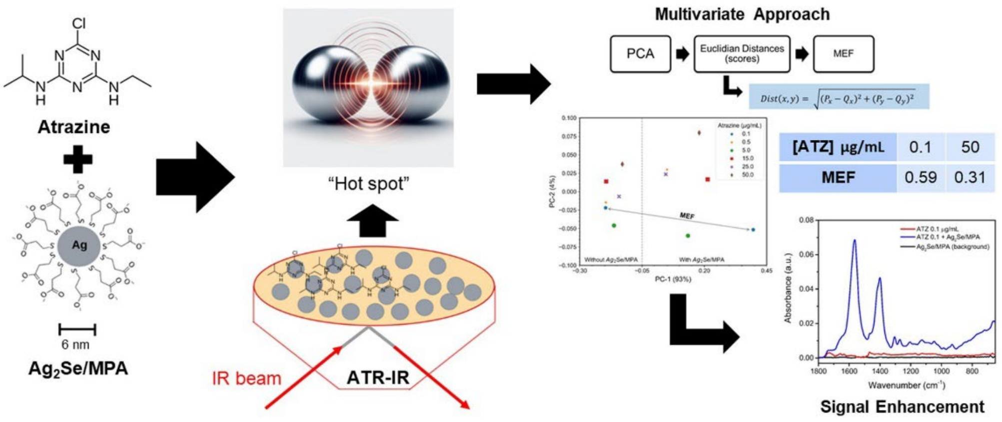

**Figure 3.** A surface-enhanced infrared absorption spectroscopy (SEIRA) multivariate approach for atrazine detection [96].

In the development of SEIRA substrates based on metallic nanomaterials, Gong et al. achieved a breakthrough in pesticide detection by fabricating a silver nanoparticle-coated copper foam (AgNP/Cu foam) substrate—a well-designed metallic nanostructure that significantly enhances the infrared signals of target molecules. In the detection of thiram, this approach reduced the limit of detection (LOD) to 0.024 mg·$mL^{-1}$, representing an improvement of two orders of magnitude over conventional infrared spectroscopy. Furthermore, the method enables precise identification of molecular fingerprint features, such as the characteristic absorption peak at 1236 $cm^{-1}$.

The innovation lies in its transmission-mode SEIRA (T-SEIRA) configuration combined with a three-dimensional porous substrate design. This architecture ingeniously overcomes the inherent limitation of poor transparency in metallic materials, enabling rapid, in-situ detection without complex sample pretreatment. In contrast, traditional infrared spectroscopy is severely constrained by background interference at low concentrations and cumbersome sample preparation procedures. These distinct advantages clearly highlight the transformative potential of SEIRA technology in the field of pesticide analysis [97].

### SEIRA Substrates Based on Hybrid Perovskites

In recent years, hybrid organic-inorganic perovskites (HOIPs) have emerged as promising materials in optoelectronics and sensing due to their excellent photoelectric properties and tunable bandgaps (1.3–1.7 eV) [98]. Their unique semiconductor characteristics—such as high charge carrier mobility and strong plasmonic effects—offer a new class of low-cost, highly sensitive substrates for surface-enhanced infrared absorption spectroscopy (SEIRA) [99].

Studies have demonstrated that, through rational design and optimization, perovskite-based substrates exhibit outstanding performance in pesticide residue detection, advancing the capabilities of trace-level analytical techniques. In SEIRA applications, $CH_3NH_3PbX_3$ (X = Cl, Br, I) thin films have been innovatively employed as enhancing substrates. These uniform and stable films are fabricated via solvent evaporation or spin-coating followed by annealing (100 °C for 45 min). Characterization results confirm their good thermal stability and typical semiconductor behavior. The synergistic effect of surface plasmon resonance and carrier dynamics significantly enhances the infrared signals of target molecules. Comparative experiments reveal that $CH_3NH_3PbBr_3$ achieves a signal enhancement factor of up to 150 for acrylamide, outperforming $CH_3NH_3PbCl_3$ (80) and $CH_3NH_3PbI_3$ (82), indicating a strong influence of halide composition on enhancement performance. These finding highlights that the band structure and charge carrier dynamics of perovskite materials are key mechanisms governing SEIRA efficiency [99].

Leveraging these advantages, researchers have successfully applied $CH_3NH_3PbBr_3$-based substrates to the detection of pesticide residues in real samples. Using benzoyl peroxide (BPO)—a common additive in flour—as a model analyte, high-sensitivity detection was achieved at the characteristic peaks of 1759 $cm^{-1}$ and 1224 $cm^{-1}$. The method exhibited a linear detection range of 0.004–0.064 mol/L with correlation coefficients ($R^2$) of 0.9958 and 0.9975, respectively, demonstrating excellent quantitative capability. More importantly, recovery rates in real samples reached 100.4%–101.0%, with RSD no greater than 1.42%, indicating high accuracy and reproducibility. Additionally, the substrate can be regenerated through simple rinsing with acetone and reused multiple times, significantly reducing operational costs. This approach presents an efficient and economical solution for food safety monitoring [99].

To further improve detection limits and material stability, Wang et al. developed a core-shell nanostructure based on CdS-coated $CsPbX_3$ (X = Cl, Br) quantum dots (CPCBM/CdS) [100]. This design effectively addresses the inherent instability of traditional perovskites in aqueous environments, greatly enhancing durability. By introducing Mn/Br co-doping to induce spin polarization and applying external magnetic field regulation, the carrier lifetime was extended to 4244 ps—approximately 2.2 times longer than in the unmodulated system. Based on this enhanced material, a photoelectrochemical sensor was constructed by integrating microfluidic paper-based analytical devices (μ-PADs) and a DNA nanowire-based signal amplification strategy. This platform enabled ultra-sensitive detection of the neonicotinoid pesticide acetamiprid (ACE). The method achieved an exceptionally low detection limit of 23 fM, with a linear range spanning five orders of magnitude ($10^{-13.5}$ to $10^{-9}$ M). In practical tests on agricultural products such as tomatoes and cucumbers, recovery rates ranged from 90.7% to 105.6%, with RSD below 5.29%, demonstrating outstanding reliability and applicability.

In summary, hybrid perovskites have become ideal candidates for SEIRA substrate development, thanks to their tunable optoelectronic properties and significant plasmonic enhancement effects. From thin-film substrates to core-shell quantum dots, and from single enhancement mechanisms to multi-strategy synergistic designs, their application in pesticide residue detection continues to deepen and evolve. Future advancements through material engineering, surface functionalization, and device integration are expected to enable perovskite-based sensing platforms to achieve even higher sensitivity, selectivity, and broader applicability for on-site, rapid detection. These developments hold strong promise for providing robust technological support in food safety and environmental monitoring.

### Methodological Innovations and Hyphenated Techniques in SEIRA

In recent years, methodological advancements and the integration of complementary technologies have become key drivers in the development of surface-enhanced infrared absorption spectroscopy (SEIRA). Among these, the coupling of SEIRA with electrochemistry (EC-SEIRAS) and the integration of porous materials have emerged as prominent research frontiers.

EC-SEIRAS systems enable in situ monitoring of pesticide degradation pathways, offering real-time molecular-level insights into reaction mechanisms. Meanwhile, the incorporation of three-dimensional porous substrates—such as filter paper or copper foam—combined with physical filtration techniques, allows for the simultaneous enrichment and detection of pesticide residues. This synergistic approach significantly enhances sensitivity and simplifies sample handling, particularly for trace analysis in complex matrices [101].

For dithiocarbamate (DMDs) pesticides, Gong et al. demonstrated that an optimized silver nanoparticle-coated copper foam substrate achieved a 2.9-fold enhancement for thiram at 1371 $cm^{-1}$, while a gold nanoparticle-based substrate exhibited an even more remarkable 188.2-fold enhancement for ziram [102]. These results highlight the critical role of metal type and nanostructure design in maximizing SEIRA performance.

Despite significant progress, several challenges remain. Improving substrate stability under operational conditions and mitigating interference from complex sample matrices (e.g., food or environmental samples) are key hurdles for real-world deployment. Emerging materials such as phonon polariton resonators—known for their low optical losses and narrow resonance peaks—hold promise for pushing the sensitivity limits of SEIRA to new levels. Moreover, AI-driven spectral analysis algorithms are expected to play a transformative role in optimizing quantitative models. Techniques such as PLSR could be significantly enhanced through machine learning-assisted peak deconvolution, baseline correction, and multivariate calibration, leading to more robust and accurate detection.

Current research indicates that SEIRA technology is transitioning from laboratory-based studies toward field-deployable, rapid detection systems. With ongoing advances in material design, method integration, and data analytics, SEIRA is evolving into a powerful, portable, and efficient solution for pesticide residue monitoring—offering strong support for regulatory compliance and public health protection.

## *2.3. Fluorescence Spectroscopy*

### 2.3.1. Principle

Fluorescence spectroscopy is an analytical method that detects characteristic fluorescence signals from pesticide molecules when excited by light of a specific wavelength. The principle involves molecules absorbing light energy, causing electronic transitions, and emitting fluorescence at a shifted wavelength as they return to the ground state. Quantitative detection is achieved by analyzing the fluorescence intensity and characteristic spectral lines [103,104]. This technique is noted for its simplicity, speed, high sensitivity, selectivity, and ability to provide extensive molecular information about the substances being tested, making it particularly suitable for detecting trace substances.

The technology is primarily divided into three types based on spectral type: front-face fluorescence spectroscopy (for direct detection of solid sample surfaces), synchronous fluorescence spectroscopy (simultaneously scanning excitation and emission wavelengths), and three-dimensional fluorescence spectroscopy (providing excitation-emission matrix information). Three-dimensional fluorescence can acquire richer molecular structure data. In terms of detection methods, there are three categories: direct detection is suitable for naturally fluorescent pesticides like carbendazim, with detection limits reaching 0.005 mg/kg; derivatization enhances non-fluorescent pesticide signals through chemical modifications, common markers include dansyl chloride and quantum dots; probe methods utilize molecular recognition mechanisms such as aptamers and imprinted polymers for specific sensing. The advantages include ultra-high sensitivity (2-3 orders of magnitude higher than chromatography), rapid detection ($<3$ minutes), and a trend towards portability. However, it has three main limitations: only 35% of pesticides have intrinsic fluorescence; matrix interference results in a false positive rate as high as 22%; and it cannot detect systemic pesticide residues [105]. Recent advancements involve time-resolved fluorescence (with lifetime differences $>10^6$ folds) to eliminate background interference, and the combination of three-dimensional fluorescence with chemometrics for simultaneous analysis of multiple components [106].

Research has found that traditional fluorescence detection relies on Stokes shift (emission wavelength longer than excitation wavelength), while novel fluorescence systems introduce upconversion fluorescence and ratiometric fluorescence modes by regulating interactions between luminescent materials and targets [107,108]. Upconversion fluorescence employs rare-earth doped nanoparticles (e.g., $NaYF_4$:$Yb^{3+}$, $Er^{3+}$) with multiphoton absorption characteristics to convert NIR light (like 980 nm) into visible light emissions, effectively avoiding interference from autofluorescence of biological tissues [109]. Additionally, upconversion fluorescence probes, through surface modifications with aptamers or MIPs, can specifically recognize organophosphorus pesticides (OPPs) [110]. Ratiometric fluorescence constructs dual-emission probes (e.g., silicon-carbon dots combined with gold nanoclusters) using the intensity ratio of two fluorescence peaks as the detection signal, reducing errors caused by light source fluctuations and probe concentration, significantly enhancing detection stability. These innovations address traditional fluorescence detection's low sensitivity and poor anti-interference capabilities, offering solutions through material design and signal processing innovations [111,112].

### 2.3.2. Applications of Fluorescence Spectroscopy in Pesticide Residue Detection

Fluorescence spectroscopy coupled with advanced data analysis techniques has demonstrated significant advantages in the detection of pesticide residues. Wang et al. developed a method for detecting carbamate pesticide residues (clothianidin and carbaryl) in tomatoes based on excitation-emission matrix (EEM) fluorescence combined with a back-propagation (BP) neural network optimized by a mind evolutionary algorithm (MEA-BP). By dynamically matching the characteristic vibrational peaks of pesticides within the 8–12 μm wavelength range (e.g., P=O bond at 1240 $cm^{-1}$) using an electrostatic gating technique and enhancing the signal with complex frequency waves (CFW), the method achieved a detection range of 0.01–1.00 μg $mL^{-1}$, with limits of detection as low as 0.147 μg $mL^{-1}$ for clothianidin and 0.159 μg $mL^{-1}$ for carbaryl. The average recovery rates ranged from 98.94% to 99.25%. The MEA-BP model outperformed the traditional BP network, reducing iteration time by 36% (304 iterations), decreasing mean square error by 66% (to 0.0057), and increasing the correlation coefficient to 0.99873. The study further validated that soaking in a sodium bicarbonate solution for 12 minutes was the most effective method for pesticide removal, reducing residue levels to 30.21%–37.96%. This approach provides a highly sensitive, low-cost solution for food safety monitoring [113].

### Application of NIR Fluorescent Probes in the Detection of Organophosphorus Pesticides

Alongside breakthroughs in conventional pesticide detection methods, the rapid development of NIR fluorescent probe technology has opened new avenues for detecting organophosphorus pesticides. Yi et al. developed a NIR fluorescent probe (Probe 1) based on a hemicyanine scaffold, in which hydroxyl groups were acylated with acetyl chloride and a fluorescence quenching group was introduced. The probe leverages the specific hydrolysis of ester bonds by carboxylesterase (CES), releasing a fluorophore that emits at 710 nm, thereby enabling the detection of OPPs [78]. The probe achieves a detection limit of 0.1734 μg/L for propoxur, with a linear range of 0–10 μg/L, and spiked recovery rates in cabbage samples ranging from 97.63% to 100.21% (RSD < 5.62%). Furthermore, Probe 1 has been successfully applied to real-time imaging in live cells (HeLa cells) and Staphylococcus aureus, demonstrating excellent sensitivity (detection limit of 0.0562 mU/mL for CES), high selectivity (stable performance within pH 6–7.5 and 36–40 °C), and outstanding biocompatibility (cell viability > 85%) [114].

Meanwhile, Zheng et al. designed a novel NIR fluorescent probe, PT-CES, based on a 4-[4-(dimethylamino)styryl] pyridinium scaffold and employing an ester hydrolysis mechanism. By harnessing an intramolecular charge transfer (ICT) effect, the probe enables ultrafast response to organophosphorus pesticides. It reaches signal stability within 30 minutes in PBS buffer, with a detection limit of 0.00396 mU/mL for CES. The detection range for dichlorvos (DCP) and trichlorfon extends up to 0–150 μg/L, with detection limits of 18.90 μg/L and 16.53 μg/L, respectively. Recovery rates in vegetable samples remain stable between 96.5% and 102.7%. PT-CES has not only been successfully used to detect pesticide residues in cucumbers but also validated through cellular co-localization experiments for its ability to target CES in mitochondria, enabling dynamic monitoring of CES activity in liver tissues. This provides an efficient and reliable analytical tool for both food safety and biomedical research [115].

In comparison, Probe 1 developed by Yi et al. achieves ultra-low-concentration detection of propoxur, while PT-CES designed by Zheng et al. exhibits superior response speed and a broader linear detection range. These technological advances not only offer new strategies for rapid, on-site detection of pesticide residues but also expand the potential applications in live-cell imaging and monitoring of enzyme activities related to diseases.

### Application of Fluorescent Probes Based on Novel Functional Materials in Pesticide Detection

In recent years, the rapid development of novel functional materials such as nanomaterials, metal-organic frameworks (MOFs), quantum dots, and metallic nanoparticles has opened up innovative pathways for the design and performance enhancement of fluorescent probes [116–118]. Against this backdrop, Xu et al. developed a wearable glove sensor based on carboxymethyl cellulose (CMC) aerogels integrated with dual fluorescence centers (EuMOFs red fluorescence/carbon dots blue fluorescence). This sensor employs a ratiometric fluorescence strategy to achieve non-invasive detection of OPPs. The sensor is fabricated using a post-synthetic cation exchange method to produce EuMOFs with high fluorescence quantum yields (38%), which are then co-loaded with carbon dots that provide stable reference signals into a porous CMC aerogel matrix. The detection principle is based on the competitive adsorption between EuMOFs and the target compound chlorpyrifos (CP). Carbon dots serve as an internal reference signal to correct for environmental interference. The sensor responds within 30 seconds, achieving a detection limit for CP on agricultural product surfaces as low as 89 nM, with a linear range of 5–40 μM. Actual sample tests demonstrated excellent recovery rates (96.5%–102.7%) and robust interference resistance. Notably, as pesticide concentrations increase, the sensor's fluorescence color shifts visibly from red to blue, observable by the naked eye. Combined with a portable UV lamp, this allows for on-site interpretation. Featuring flexible, bendable design, high accuracy ($R^2 = 0.99529$), and real-time detection capability, this device offers an innovative solution for food safety monitoring, integrating portability, sensitivity, and visual readability [119].

This advancement not only highlights the potential of integrating advanced functional materials into practical sensing devices but also underscores the importance of developing user-friendly tools for rapid, on-site analysis. The combination of high sensitivity, ease of use, and visual feedback makes this sensor particularly valuable for field applications in ensuring food safety and quality.

In addition to carbon dots, noble metal nanomaterials have also demonstrated unique advantages in pesticide detection. Wang et al. developed a colorimetric method based on the aggregation of unmodified gold nanoparticles (AuNPs) for the visual determination of total residues of nereistoxin-based insecticides. In this approach, various nereistoxin analogs in samples are first converted into nereistoxin—a bifunctional molecule containing both amino and thiol groups—through liquid-liquid extraction and alkaline hydrolysis. These functional groups can specifically bind to 13 nm citrate-stabilized AuNPs via electrostatic interactions and Au–S covalent bonding, inducing nanoparticle aggregation and a distinct color change from wine red to blue, clearly visible to the naked eye within the concentration range of 50–250 μg/kg. Quantitative analysis is achieved by measuring the absorbance ratio at 660 nm and 519 nm ($A_{660}/A_{519}$), with a detection limit of 40 μg/kg and a linear range of 50–250 μg/kg ($R^2 = 0.9953$). The entire assay is completed within 3 minutes. Spiked recovery tests in real samples such as tea and kiwifruit yielded results between 61.1% and 105%, with coefficients of variation (CV) ≤10.9%, indicating reliable performance. When used in conjunction with a standard colorimetric chart, the method enables semi-quantitative visual detection, meeting Japan’s maximum residue limit (MRL) of 100 μg/kg for these pesticides. This strategy requires no expensive instrumentation, is simple to operate, and combines rapidity, low cost, and high specificity, showing strong potential for on-site applications [120].

### Application of Fluorescence Sensors Based on Functional Materials in Pesticide Detection

Fluorescence spectroscopy technology has shown significant development potential and diversity in pesticide detection research, with key highlights being high sensitivity, rapid response, and good practical applicability [2,12]. Particularly through the integration of nanomaterials—such as gold nanoparticles and up-conversion fluorescent materials—with biological recognition elements like aptamers, it has achieved specific capture and signal amplification for trace pesticides [121].

Based on the different sensing materials, these sensors can be mainly categorized into four types: enzyme-based fluorescent sensors, metal-organic framework (MOFs) sensors, graphene oxide-based sensors, and organic molecule sensors [122,123]. Enzyme-based fluorescent sensors combine biological enzymes such as carboxylesterase (PvCarE1) and alkaline phosphatase (ALP) with nanomaterials like gold nanoclusters. By utilizing enzyme inhibition principles, they achieve detection of organophosphorus pesticides, offering high recovery rates and low detection limits. These sensors also provide semi-quantitative visualization capabilities. MOFs sensors leverage the tunable pore structures of MOFs and mechanisms such as fluorescence resonance energy transfer (FRET) for pesticide detection. However, their preparation processes are relatively complex, requiring precise control over synthesis conditions. Graphene oxide-based sensors exploit the strong fluorescence quenching performance of graphene oxide (GO) or reduced GO (r-GO). They achieve detection through the adsorption and subsequent release of aptamers. Additionally, these sensors can be integrated with smartphone platforms to facilitate portable and on-site analysis. Organic molecule sensors are designed by coupling fluorophores, such as BODIPY, with recognition groups. They utilize photophysical mechanisms like photoinduced electron transfer (PET) to achieve highly selective detection. Some of these sensors have been further developed into test strips for field-deployable visual detection. Current challenges focus on material stability, large-scale production, and optimization of biocompatibility. Future directions will concentrate on integrating multiple technologies and expanding practical application scenarios. These advancements not only enhance the sensitivity and specificity of pesticide detection but also pave the way for developing more robust, user-friendly tools that can be widely applied in food safety monitoring and environmental protection.

Enzyme-based fluorescent sensors represent a typical paradigm of combining biological recognition with nanomaterials. Wang et al. developed a fluorescence sensor based on recombinant CES PvCarE1 and glutathione-stabilized gold nanoclusters (GSH-AuNCs) for the rapid detection of organophosphorus pesticides (OPPs). The GSH-AuNCs were synthesized via a high-temperature reduction method, with an average particle size of 3.1 nm and exhibiting fluorescence at 630 nm when excited at 400 nm. The detection principle is based on OPs inhibiting the catalytic activity of PvCarE1 on p-nitrophenyl acetate (p-NPA), which hydrolyzes to produce p-nitrophenol (p-NP), quenching the fluorescence of GSH-AuNCs through an inner filter effect. Under optimized conditions (pH 7.5, 25°C), the sensor achieved detection limits of 0.2 μg/L for DCP, 5 μg/L for trichlorfon, and 5 μg/L for profenofos, with linear ranges spanning from 0.2 to 200 μg/L to 5 to 1000 μg/L. In spiked apple samples, recoveries ranged from 84.5% to 106.3%, with RSD of 1.3% to 10.5%, demonstrating good accuracy and practicality [124].

Wei et al. reported a fluorescence sensor based on ALP-triggered in situ reactions for highly sensitive detection of OPPs. The material preparation involves ALP catalyzing the dephosphorylation of substrate AAP to generate ascorbic acid, which subsequently reacts with o-phenylenediamine (OPD) to form a fluorescent product, DFQ. The analytical method leverages the principle that OPPs inhibit ALP activity, leading to a decrease in fluorescence signals, detected via fluorescence spectroscopy (excitation/emission wavelengths: 360/425 nm). Detection performance showed a linear range of 20 pg/mL to 1000 ng/mL for chlorpyrifos, with a detection limit of 15.03 pg/mL (S/N=3), outperforming most reported methods. In practical applications, the spiked recovery rates for leek and celery samples were between 94.5% and 106.7%, with RSD below 11.51%, validating the accuracy and reliability of the method. This sensor does not require synthesis of nanomaterials or complex labeling and can achieve semi-quantitative visual detection through changes in solution color under UV light [125].

Qvortrup et al. reviewed fluorescence-based detection methods for OPPs, focusing on the construction of ALP-triggered reaction-based fluorescence sensors. Material preparation involves ALP catalyzing the conversion of substrate AAP into AA, which reacts with OPD to form the fluorescent product DFQ (emission peak at 425 nm). OPPs reduce fluorescence signals by inhibiting ALP activity. Analytical methods indicated that the sensor has a linear range of 20 pg/mL to 1000 ng/mL for chlorpyrifos, with a detection limit as low as 15.03 pg/mL (S/N=3), surpassing most reported methods. In actual samples (leek, celery), recovery rates reached 94.5% to 106.7%, with RSD below 11.51%, and it also features semi-quantitative UV colorimetric functionality. This method does not require complex labeling or expensive instruments, achieving high sensitivity and visual detection through changes in fluorescence intensity and color [126].

Fu et al. reviewed sensors for detecting OPPs based on ALP-triggered in situ fluorescence reactions. Through ALP catalyzing the conversion of AAP to AA, which then reacts with OPD to form the strong fluorescent product DFQ (425 nm), OPPs reduce fluorescence intensity by inhibiting ALP activity. Under optimized conditions, the sensor had a linear detection range of 20 pg/mL to 1000 ng/mL for chlorpyrifos, with a detection limit as low as 15.03 pg/mL and recovery rates of 94.5% to 106.7% (RSD < 11.51%). This method does not require complex labeling or costly equipment and enables semi-quantitative detection through color changes under UV light, successfully applied to detect chlorpyrifos in leeks and celery, showcasing high sensitivity, broad detection range, and good applicability to real samples [127]. These enzyme-based sensors demonstrated good recovery rates of 84.5% to 106.7% in practical agricultural product testing, with RSD generally below 11.51%, verifying their reliability.

MOF sensors have garnered significant attention due to their tunable pore structures and surface properties. Tu et al. reviewed the research progress of non-biological fluorescence sensors in pesticide detection, with a focus on summarizing sensor designs based on organic small molecules, MOFs, and nanomaterials. The material preparation methods include the synthesis of organic ligands, construction of MOFs (such as Zr-MOF and ZnPO-MOF), and quantum dot functionalization (e.g., CdTe QDs combined with thiourea). Analytical methods primarily rely on fluorescence enhancement/quenching mechanisms, such as PET and FRET. In terms of detection performance, these sensors exhibit high sensitivity towards various pesticides; for instance, Zr-MOF achieved a detection limit as low as 0.456 nM for methyl parathion, while CdTe QD sensors reached a detection limit of 0.1 nM for chlorpyrifos. Recovery rates in real samples (such as water and vegetables) were generally above 90%, with ZnPO-MOF showing recovery rates consistent with chromatographic results when detecting methyl parathion in irrigation water [128].

For example, Wang et al. innovatively constructed a biomimetic fluorescence sensing system based on palladium metal-MOFs (Pd-MOF). Nanoprobes with an average size of 260 nm were prepared through thermal polymerization, featuring a microporous structure of 2.0 nm and an ultranarrow bandgap of 0.025 eV, which endows the system with molecular recognition capability for phorate. Upon target binding within the pores, P-π conjugation increases the bandgap to 0.046 eV, triggering fluorescence enhancement at 612 nm, achieving an ultra-low detection limit of 0.0017 ppb (a 20-fold improvement over national standards). This probe completes detection within 45 seconds, with recovery rates ranging from 87.69% to 106.12% in tap water and agricultural product samples. XANES spectroscopy and density functional theory confirmed the coordination mechanism between Pd and phorate. A biomimetic-designed test strip further enables rapid visual detection, offering a new solution for pesticide residue monitoring [129]. These sensors combine rapid response (within two minutes) and high selectivity but face challenges such as complex preparation processes or matrix interference for some materials. Future work should focus on optimizing stability and practicality. These advancements not only enhance the sensitivity and specificity of pesticide detection but also pave the way for developing more robust, user-friendly tools that can be widely applied in food safety monitoring and environmental protection.

GO and reduced graphene oxide (r-GO) based sensors have become a research hotspot due to their excellent fluorescence quenching performance. Sun et al. reviewed the application of fluorescence sensors based on GO and r-GO in the safety detection of aquatic products. The material preparation primarily involves methods such as the Hummers method for GO and chemical reduction, plasma reduction for r-GO. r-GO exhibits stronger fluorescence quenching capabilities due to its higher $sp^2$ hybridized regions. Analytical methods are based on the principle of FRET, where fluorescently labeled aptamers interact with GO/r-GO through adsorption-desorption to detect target molecules. For pesticide detection, sensors achieved detection limits as low as 0.14 ppb (pure chlorpyrifos) and 2.05 ppb (commercial formulation). Detection of diazinon using upconversion nanoparticles modified aptamers reached a limit of 0.023 ng/mL, suitable for environmental and agricultural samples. Some sensors integrate with smartphone platforms or test strips for portable detection; for instance, $Cd^{2+}$ detection using a fluorescent test strip combined with a smartphone has a detection limit of 0.1 mM. Recovery rates were satisfactory for PQ fluorescence quenching sensors in actual water samples, while Fe-GQDs sensors can be reused via magnetic separation, though specific recovery rate data were not explicitly mentioned in the literature. Overall, GO/r-GO sensors exhibit high sensitivity, selectivity, and practicality, although large-scale production and biocompatibility still require optimization [130].

Yu et al. further reviewed the use of GO and r-GO-based fluorescence sensors in the safety detection of aquatic products. Material preparation methods include Brodie, Staudenmaier, and Hummers methods for synthesizing GO, along with chemical reduction, thermal reduction, and plasma reduction techniques for producing r-GO. Analytical methods leverage the fluorescence quenching properties of GO/r-GO based on FRET principles. Fluorescently labeled aptamers bind to target molecules, leading to the recovery of fluorescence signals for detection. In pesticide detection, sensors demonstrated detection limits as low as 0.13 nM to 4 ng/mL for OPPs like DCP and diazinon, with good recovery rates. Diazinon detection was applicable to both environmental and agricultural samples [131]. However, large-scale production and biocompatibility remain significant bottlenecks limiting their widespread application.

These advancements highlight the potential of GO and r-GO-based sensors for achieving high sensitivity and specificity in pesticide detection, but challenges such as scalability and biocompatibility need to be addressed to fully realize their potential in practical applications. These sensors offer promising solutions for enhancing food safety monitoring and environmental protection, provided that future research focuses on optimizing these aspects.

Organic molecule sensors have achieved highly selective detection through sophisticated molecular design. Sharma et al. reviewed various organic fluorescent sensors for pesticide detection. In terms of material preparation, the primary strategy involves coupling fluorophores—such as rhodamine, BODIPY, and naphthalimide—with specific recognition groups (e.g., hydroxamic acid, oxime) to enable detection via photophysical mechanisms like PET and ICT. The analytical approach relies on phosphorylation reactions that trigger changes in fluorescence signals; for example, a βhydroxyoxime sensor undergoes cyclization to form an isoxazole, resulting in fluorescence enhancement, while BODIPY derivatives achieve signal amplification by restricting C-Ar bond rotation. These sensors exhibit excellent performance: a naphthalimide-based probe achieves a detection limit of 0.52 μM for fluoride ions, and a BODIPY sensor detects DCP down to 20.7 ppb. In agricultural products, certain sensors demonstrate recovery rates of 94.5%–106.7% with RSD < 11.51%. Integration with test strip technology further enables visual, on-site detection [132]. Despite challenges related to complex synthesis, the tunable nature of their molecular structures offers broad opportunities for developing novel pesticide sensors.

### Advances in Multimodal Pesticide Residue Detection Based on Fluorescence Spectroscopy

Recent studies have demonstrated that integrating fluorescence spectroscopy with other techniques can significantly enhance detection performance. Fen et al. developed a CES fluorescent probe (Probe 1) based on a benzothiazole fluorophore and a phenyl dimethylcarbamate recognition group for the rapid detection of carbamate pesticides. The probe was synthesized via a two-step organic route with a 79% yield. It operates through the enzymatic hydrolysis of the ester bond in the probe by CES, releasing the fluorescent benzothiazole moiety (emission at 436 nm). The system responds within 25 minutes in pH 7.0 buffer, achieving a detection limit of 0.02703 U/mL for CES. By employing a competitive enzymatic inhibition mechanism, the probe exhibits high sensitivity toward the representative carbamate pesticide carbaryl, with a detection limit of 27.40 nM and a linear range of 0–1.0 μM, along with excellent selectivity against 16 potential interfering substances. In real-sample analyses of fruit juices and vegetable juices, recovery rates ranged from 97.85% to 103.10% (RSD < 1.44%). Notably, the method was innovatively coupled with smartphone-based RGB analysis, enabling visual quantification of a solution color gradient (from light to deep blue) by the naked eye. This approach provides a field-deployable, equipment-free solution for rapid on-site detection [133].

It is worth noting that while fluorescent probe technologies based on enzymatic hydrolysis enable efficient detection of individual pesticides, they remain limited in the simultaneous analysis of multiple pesticide residues. Bian et al. developed a multi-pesticide residue detection method by combining fluorescence spectroscopy with a PLS regression model, overcoming the traditional limitation of conventional fluorescence techniques—which typically allow detection of only one analyte due to overlapping emission spectra. The study selected four pesticides with highly overlapping fluorescence signals: zhongshengmycin, paclobutrazol (PBZ), boscalid, and pyridaben. By preparing 151 mixed samples with varying concentrations (e.g., zhongshengmycin: 0–0.0305 mg/mL, pyridaben: 0–0.0033 mg/mL), multiple PLS models were established. The approach (1) utilized a seven-principal-component model; after cross-validation and removal of outliers, the model achieved $R^2$ values ranging from 0.9827 to 0.9913, with recovery rates approaching the theoretical value of 1; (2) eliminated the need for complex sample pretreatment, enabling simultaneous, non-destructive detection of multiple pesticides in water samples; and (3) achieved RMSE as low as 0.000107–0.000996 mg/mL, indicating sufficient sensitivity for real-world applications. This strategy provides a rapid, cost-effective approach for online water quality monitoring [134].

Further expanding the application scope to meet the growing demand for multi-pesticide residue detection in agricultural products, Zhang et al. developed an innovative high-throughput screening method by integrating fluorescent labeling with immunoassay technology, making it more suitable for complex matrices (Figure 4). Specifically, they reported a traffic-light-inspired fluorescent lateral flow immunoassay (T-FLFIA) for the simultaneous detection of multiple pesticide residues. Through a self-assembly approach, three distinct fluorescent aggregation-induced emission nanoparticles (AIENP@Ni/EC) emitting green, yellow, and red light were synthesized. These nanoparticles, with an average size of 155–188 nm, feature a core structure composed of AIEgens encapsulated within a nickel-epicatechin (Ni/EC) metal–polyphenol network. Antibodies were then conjugated to the nanoparticles via electrostatic adsorption to form immunoprobes. Leveraging a competitive immunoassay format, the method enables simultaneous detection of chlorothalonil

(CTN), paclobutrazol (PBZ), and fipronil (FIP) within 5 seconds, with linear ranges of 0.05–100, 0.05–250, and 0.05–10 ng/mL, respectively, and detection limits as low as 0.038, 0.025, and 0.046 ng/mL. In spiked real samples (apple and cowpea), recovery rates ranged from 90.2% to 114.0%, with a qualitative accuracy of 92.5%. Compared to traditional gold nanoparticle-based methods, the sensitivity was improved by 3.37- to 5.52-fold. The method also demonstrated high specificity—no cross-reactivity with 12 potential interfering substances—and strong resistance to matrix effects [135].

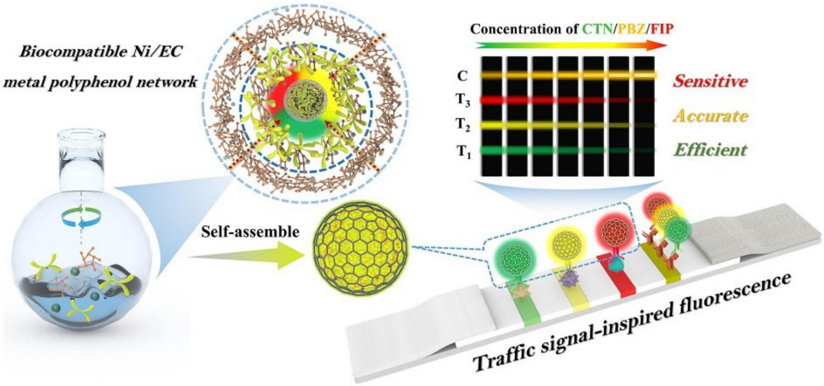

**Figure 4.** Traffic signal-inspired fluorescence lateral flow immunoassay utilizing self-assembled AIENP@Ni/EC for simultaneous multi-pesticide residue detection [135].

Compared to infrared spectroscopy, research on fluorescence spectroscopy is still relatively limited and faces several challenges. Fluorescence spectroscopy can only detect substances that are intrinsically fluorescent, which significantly restricts its application scope. For non-fluorescent analytes, the method requires the addition of fluorescent reagents or derivatization reactions to generate a detectable signal, adding complexity and difficulty to pesticide residue analysis. Furthermore, fluorescence signals are highly susceptible to environmental factors such as solvent composition, pH, and temperature, which can affect fluorescence intensity and stability, potentially leading to inaccurate measurements. These limitations hinder the robustness and reproducibility of the technique. Consequently, substantial research and development efforts are still needed before fluorescence spectroscopy can be widely adopted in practical, real-world applications.

### 2.3.3. Comparison of Various SERS Detection Methods based on Fluorescence spectrum

Table 2 highlights the diverse performance characteristics of various fluorescence spectroscopy-based methods in pesticide residue analysis. Fluorescence spectroscopy combined with biosensing technology demonstrates high recovery rates of 98.7–109.2% and an extremely low detection limit of $<1.2\times10^{-12}$ M for pesticides such as paraoxon and chlorpyrifos, with a detection time under 20 minutes, making it suitable for rapid detection of multiple pesticide classes [105]. For FIP, a fluorescent immunosensor achieved recoveries of 95.95–137.07%, a detection limit of 0.01 μg/L, and exceptionally high precision (RSD 0.07–0.23%) [110]. A biomimetic fluorescent sensor exhibited recoveries of 87.69–106.12% for demeton-S-methyl, a detection limit of 0.0017 μg/L, and a response time of only 45 seconds, combining high sensitivity with rapid analysis [99]. EEM fluorescence spectroscopy yielded recovery rates close to 99% for insecticides TSU and CBL, with detection limits of 0.147 and 0.159 μg/mL, respectively [114].

NIR fluorescent probes showed recoveries of 97.63–100.21% for isocarbophos, with RSDs of 2.32–5.62% and a detection limit of 0.030 μg/L [110]. Another NIR method reported recoveries of 96.50–101.83% for DCP and 97.09–102.71% for trichlorfon, although with higher detection limits (approximately 16–19 μg/L) [116]. Dual-signal fluorescence assays achieved an RSD ≤12% for chlorpyrifos, with a detection limit of $89\times10^{-9}$ M and a response time of just 30 seconds [120]. Turn-on fluorescence methods enabled detection of DCP, trichlorfon, and profenofos within minutes, with recoveries ranging from 84.5% to 106.3% and detection limits of 0.2, 5, and 5 μg/L, respectively [124].

Although traditional fluorescence spectroscopy can take up to 180 minutes, it achieves a remarkably low detection limit of 0.015 ng/mL for chlorpyrifos, with stable recoveries of 94.5–106.7% [125]. Conversely, for demeton-S-methyl, this method reached an ultra-low detection limit of 1.7 pg/L within 45 seconds, underscoring its potential for high sensitivity [129]. Dual-excitation colorimetric techniques allow simultaneous detection of four pesticides—including atrazine and carbaryl—within 5 minutes, with all recoveries exceeding 95% and RSDs below 3.5% [131]. Smartphone-based image recognition offers field-deployable convenience, achieving a detection limit of $27.40\times10^{-9}$ M for carbaryl and recoveries of 97.85–103.10% [120]. The integration of PLS models with fluorescence spectroscopy is well-suited for online monitoring, supporting a broad concentration range (0–0.0305 mg/mL) [134]. Multicolor fluorescent signaling methods achieve detection limits as low as 0.025–0.046 ng/mL for CTN, PBZ, and FIP, with response times under 5 seconds, demonstrating exceptional speed and ultrahigh sensitivity [135]. Overall, these methods continue to improve in sensitivity, speed, and portability, providing diverse solutions for pesticide residue detection.

## *2.4. UV-Vis Spectroscopy*

### 2.4.1. Principle

UV-Vis spectroscopy is an analytical technique based on the selective absorption of electromagnetic radiation in the 200–800 nm wavelength range by molecules. The fundamental principle involves electronic transitions of valence electrons (σ, π, or n electrons) within a molecule, which absorb photons of specific energy and undergo transitions between electronic energy levels, such as $\sigma\rightarrow\sigma^*$, $n\rightarrow\sigma^*$, $\pi\rightarrow\pi^*$, or $n\rightarrow\pi^*$. These transitions generate characteristic absorption spectra [136,137]. The UV-Vis region is typically divided into near-ultraviolet (200–400 nm), visible (400–800 nm), and far-ultraviolet (10–200 nm, requiring vacuum conditions for detection). Transitions such as $\pi\rightarrow\pi^*$ and $n\rightarrow\pi^*$ commonly produce absorption bands in the near-UV to visible region, making them particularly useful for the analysis of organic compounds [52,138].

In pesticide residue detection, the UV-Vis spectroscopic methodology primarily comprises three approaches: UV spectrophotometry, derivatization-based colorimetric methods, and enzyme inhibition assays, forming a multidimensional and synergistic detection framework. Spectrophotometry enables rapid screening through the characteristic absorption of target molecules, derivatization enhances sensitivity via chemical reactions, and enzyme inhibition improves specificity through biochemical recognition. Current research focuses on enhancing performance through nanomaterials, integration with microfluidic systems, and the development of intelligent detection devices, leading to significantly lower detection limits (reaching μg/kg levels), shorter analysis times (≤15 minutes), and improved suitability for on-site applications. These three methodologies complement each other, collectively addressing challenges such as matrix interference and poor enzyme stability, thereby providing multi-tiered solutions for pesticide residue monitoring.

### 2.4.2. Applications of UV-Vis Spectroscopy in Pesticide Detection UV Spectrophotometry

UV-Vis spectroscopy is a vital analytical tool in pesticide detection, relying on either the characteristic absorption of target compounds at specific wavelengths or the chromogenic effects of their reaction products. Due to its wide instrument availability, methodological versatility, and cost-effectiveness, this technique meets diverse analytical needs ranging from precise laboratory analysis to rapid on-site screening. With technological advancements, modern UV-Vis methods have achieved significant improvements in sensitivity and selectivity through the synergistic design of optical signals with chemical or biological reactions, offering standardized solutions for pesticide residue monitoring.

Specifically, UV spectrophotometry has proven effective for pesticide residue screening in tea, owing to its simple instrumentation, low cost, and rapid analysis (approximately 30 minutes per test). Chen et al. developed an ultrasound-assisted extraction combined with UV spectrophotometry for the highly sensitive detection of orthophenylphenol residues in tea, achieving a detection limit of 0.12

μg/g. The method demonstrated a linear range of 0.5–20 μg/mL and spike recovery rates of 90.1%–91.2%, meeting the requirements for quantitative analysis. Compared to traditional chromatographic methods, this approach eliminates the need for complex sample preparation and expensive equipment, reducing the cost per sample by 65%. Furthermore, the coefficient of variation across six types of tea samples was less than 5%, demonstrating both rapid screening capability (30 min per sample) and accurate quantification. This cost-effective and efficient method provides a practical solution for agricultural product safety supervision [139].

Yu et al. prepared 84 apple juice samples spiked with varying concentrations of imidacloprid, acetamiprid, and thiamethoxam, and employed UV spectroscopy (200–350 nm) combined with a sparrow search algorithm-optimized backpropagation neural network (SSA-BPNN) for simultaneous detection of these neonicotinoid pesticides. UV-Vis spectra were collected using a spectrophotometer and preprocessed with Savitzky-Golay smoothing to reduce noise before model construction. The results showed that the SSA-BPNN model outperformed other models (ELM, BPNN, PSO-BPNN), achieving determination coefficients ($R^2$) of 0.9985–0.9994 and RMSE of 0.0501–0.0609 mg/L in the prediction set. The method requires no complex sample pretreatment and achieves detection limits below 0.6 mg/L (lowest tested concentration), making it suitable for rapid screening of multiple pesticide residues in apple juice. This approach offers an efficient and low-cost analytical solution for food safety monitoring [140].

Notably, the characteristic absorption of the P=O bond in OPPs at 210–230 nm provides a theoretical basis for their detection via UV spectrophotometry, enabling analysis within 5 minutes. However, this method is susceptible to matrix interference. Dong et al. developed an innovative chromogenic reaction system that enables simultaneous and accurate determination of OPPs such as methamidophos, omethoate, and dimethoate. The method exhibited a linear detection range of 0.1–10 mg/kg ($R^2 > 0.99$) and consistent spike recovery rates of 88.2%–92.5% (RSD < 3.0%). Sensitivity was improved by 40% compared to traditional test strip methods. The procedure significantly simplifies sample preparation, reducing the analysis time to 15 minutes per sample and lowering overall costs by 70%. Particularly suitable for large-scale screening in grassroots laboratories, this method combines rapid response, economic efficiency, and reliable results. It has been successfully applied to the testing of 120 batches of commercially available vegetables, demonstrating its feasibility and practicality as a technical solution for agricultural product quality and safety supervision [141].（2009 碱水解 - 分光光度法快速检测有机磷农药的研究 中文已下载）

### Derivatization-Based Colorimetric Technology

Concurrently, derivatization-based colorimetric technology enables precise capture of trace-level pesticides through chemical transformation, complementing UV spectrophotometry by leveraging their respective strengths. This technique converts pesticide molecules into derivatives with distinct coloration or characteristic UV absorption via specific chemical reactions. By exploiting functional group-specific reactions, such as the condensation of carbamates with ninhydrin to form a purple-blue product, the method enhances detection sensitivity up to 0.001 mg/kg.

In recent years, significant progress has been made in the development of novel derivatizing reagents, integration with microfluidic chips, and the application of portable detection systems.

(i) Development of Novel Derivatizing Reagents

The design and synthesis of highly reactive derivatizing reagents have substantially improved detection sensitivity. For instance, 9-fluorenylmethyl chloroformate, as a newly developed derivatizing agent, exhibits three times higher reactivity than conventional reagents, enabling more efficient coupling with target pesticide molecules and achieving an exceptionally low detection limit of 0.001 mg/kg. This innovation not only enhances sensitivity but also broadens the range of detectable pesticides [142]. Additionally, broad-spectrum reagents have been explored: 2,4-dinitrofluorobenzene is effective for OPPs [142], while 5-(4,6-dichlorotriazinyl) aminofluorescein (DTAF) can be used to detect carbamate pesticides such as carbaryl.

(ii) Microfluidic Chip Integration

Microfluidic technology miniaturizes traditional batch-wise derivatization processes onto chip-based channels. By precisely controlling fluid dynamic parameters—such as flow rate and mixing time—it enables accurate regulation of derivatization reaction conditions. Recent studies demonstrate that integrating microfluidics reduces the entire derivatization-detection process from the conventional 2 hours to just 15 minutes, while improving reaction efficiency by over 40%.

(iii) Portable Detection Systems

Jiang et al. developed a supramolecular fluorescent probe, AFL@ALB, which specifically binds to pyrethroid pesticides, producing a visible "yellow-to-green" color change within 10 seconds. The method achieves a detection limit as low as 1.0773 μM, surpassing EU regulatory standards by a factor of 13. By innovatively integrating smartphone-based RGB analysis, the cost per test is reduced to merely RMB 0.5 (approximately USD 0.07), with field measurement errors below 7.2% and a total assay time of only 3 minutes. More notably, they pioneered a PBA/CNF aerogel sensor capable of real-time, visual monitoring of gaseous pyrethroids (e.g., those released from mosquito coils), achieving a detection limit of 1.7378 μM. This system establishes a technological closed-loop of "colorimetric reaction–intelligent recognition–multi-scenario adaptability," offering a portable solution with laboratory-grade accuracy for monitoring agricultural product safety and environmental health [143].

## Enzyme Inhibition Assay

UV-Vis spectroscopy plays a central role in enzyme inhibition-based pesticide detection, primarily relying on the specific inhibition of acetylcholinesterase (AChE) by organophosphorus and carbamate pesticides. The detection process involves three key steps: First, under normal reaction conditions, AChE catalyzes the hydrolysis of a substrate (e.g., acetylcholine), generating chromogenic products such as thiocholine. Subsequently, these products react specifically with the chromogenic reagent DTNB (5,5′-dithiobis-(2-nitrobenzoic acid)), forming a characteristic absorption peak at 412 nm. When target pesticides are present in the sample, they bind to the active site of AChE, thereby inhibiting its catalytic activity. By using a UV-Vis spectrophotometer to monitor real-time changes in the absorbance of the reaction system, the inhibition rate of enzyme activity can be accurately calculated, enabling quantitative analysis of pesticide residues. This approach skillfully combines the high specificity of biological recognition (>95%) with the convenience of spectroscopic detection, achieving high sensitivity down to 1 ng/mL (e.g., for glyphosate). It is particularly suitable for rapid on-site screening of complex matrices such as fruits and vegetables, providing an efficient and reliable technical solution for food safety monitoring [144,145].

The widespread application of nanozyme technology—especially graphene-based materials—offers dual advantages: an 80% reduction in detection cost and exceptional resilience under extreme environmental conditions. For example, Wei et al. developed a nanozyme sensor array based on heteroatom-doped graphene (nitrogen-doped NG, nitrogen-sulfur co-doped NSG, and GO for the detection of aromatic pesticides. NG and NSG were synthesized via a high-temperature pyrolysis method and utilized for their peroxidase-like activity to catalyze the TMB-$H_2O_2$ chromogenic reaction, with absorbance measured at 412 nm. When pesticides adsorb onto the graphene surface, they specifically inhibit the enzyme-mimicking activity, and the resulting absorbance changes are monitored by UV-Vis spectroscopy. This sensor array successfully distinguished five pesticides, lactofen, methyl fluroxypyr, bensulfuron-methyl, fomesafen, and diafenthiuron, with a detection limit as low as 5 μM, and its practicality was validated in soil samples. Molecular simulations revealed that pesticide adsorption onto active sites of graphene occurs via π-π stacking and hydrogen bonding. By combining the high stability of nanozymes with the multiplex detection capability of sensor arrays, this method provides a simple and cost-effective solution for pesticide residue detection in complex matrices [146]. Future efforts should focus on multi-enzyme cooperative recognition, nanomaterial surface modification, and optimization using machine learning algorithms to overcome limitations in detectable pesticide categories and enhance anti-interference capabilities in complex samples, thereby promoting large-scale applications in smart agriculture and food safety supervision.

However, UV-Vis spectroscopy has several limitations: it is applicable only to pesticides containing aromatic rings or conjugated systems (approximately 35% of common pesticides), while non-UV-absorbing pesticides require derivatization. Additionally, measurements are susceptible to environmental factors such as solvent polarity and pH. For instance, hydrogen-bonding effects in fenitrothion can cause shifts in absorption peaks. Current development trends include enhancing absorption signals using nanomaterials (e.g., gold nanoparticles can improve sensitivity tenfold), miniaturizing spectrometers for field-based rapid testing, and integrating with the Internet of Things (IoT) to build cloud-based spectral databases. Although UV-Vis spectroscopy is slightly less specific than fluorescence spectroscopy, its advantages of low equipment cost and operational simplicity ensure its continued importance in pesticide residue screening at grassroots and field levels.

## *2.5. HSI Technology*

### 2.5.1. Principle

Hyperspectral imaging (HSI) captures spectral information—reflectance or transmittance—across hundreds of narrow, contiguous wavelength bands from a target object, integrating this with spatial imaging to form a "three-dimensional data cube." This enables dual-dimensional analysis of both chemical composition and spatial distribution of materials [147]. Utilizing grating or prism-based dispersive systems, HSI finely segments wavelengths within the visible to NIR (Vis-NIR) spectral range (400–2500 nm), allowing simultaneous recording of continuous spectral signatures (e.g., vibrational absorption peaks of pesticide molecules) at each pixel and acquisition of the target's geometric and morphological information. Compared to conventional analytical methods, its core advantages include non-contact, non-destructive detection, high information density (simultaneous acquisition of chemical and spatial data in a single scan), and dynamic monitoring capability [148]. For instance, drone-mounted HSI systems can evaluate pesticide spray uniformity at the field scale, while whole-fruit or leaf surface residues can be spatially mapped, avoiding sampling damage and undetected blind spots [149].

### 2.5.2. Applications of HSI in Pesticide Detection

In pesticide residue detection, HSI significantly enhances detection efficiency and precision by leveraging its unique fusion of spectral and spatial information. The technology can extract characteristic spectral bands—such as the 900–1000 nm absorption features of organophosphorus pesticides—to generate two-dimensional heatmaps of pesticide concentration distribution. This enables precise localization of residue accumulation in areas such as apple stem cavities or leaf stomata, providing a visual basis for washing and sorting processes. Additionally, its early-warning capability can detect subtle spectral changes in crops under pesticide stress (e.g., red-edge shifts caused by reduced chlorophyll content), offering risk alerts for over-application before visible symptoms appear.

The core advantage of HSI lies in its ability to simultaneously capture the spatial distribution of chemical components and spectral "fingerprint" features in a single scan [150]. In contrast to traditional liquid chromatography, HSI eliminates the need for sample grinding, extraction, or chemical reagents, avoiding both sample destruction and reagent consumption. This makes it particularly suitable for online sorting of fresh agricultural products such as fruits and vegetables. Multi-band collaborative analysis further overcomes the limitations of single-spectral-feature approaches. As a result, significant research progress has been achieved in pesticide residue detection on leafy greens and other crops, including lettuce, spinach, and mulberry leaves [151,152].

For example, in detecting OPPs (e.g., chlorpyrifos) on lettuce, researchers employed a HSI system in the 400–1000 nm range. By extracting changes in reflectance at 550 nm (chlorophyll absorption valley) and 720 nm (red-edge region) and combining these with a PLS discriminant analysis (PLS-DA) model, the study successfully differentiated residue samples across a concentration gradient of 0.5–10 mg/kg, achieving a classification accuracy of 89% [153]. For pyrethroid pesticides (e.g., cypermethrin) in mulberry leaves, scholars utilized short-wave infrared spectroscopy (900–1700 nm) to capture vibrational absorption features of C-Cl bonds in pesticide molecules. Applying spectral angle mapping SAM, they successfully localized residue accumulation near leaf veins, achieving a detection limit as low as 0.2 mg/kg—10 times more sensitive than conventional enzyme inhibition assays [26].

NIR transmittance spectroscopy, with its rapid and non-destructive characteristics, has demonstrated unique advantages in identifying pesticide residues on lettuce leaves. Ge et al. innovatively fused chlorophyll fluorescence spectral data, significantly improving the accuracy of predictive models. The research team adopted a combined strategy of wavelet transform and MD-MCCV algorithms (WT-MD-MCCV) to effectively extract optimal wavelength features from spectral data. Experimental results showed that the fused model achieved a prediction accuracy of $R^2 = 0.987$ and a RMSE of only 0.005, fully validating the reliability and practical value of this technology in quantitative pesticide residue analysis [153].

The successful application of these techniques in lettuce detection has provided an important reference for pesticide residue monitoring in other crops. Researchers have since turned their attention to mulberry leaves, a key economic crop. In studies on mulberry leaf pesticide residues, Zhou et al. achieved a major breakthrough by integrating near-infrared HSI with gas chromatography. Through microscopic observation of pesticide effects using SEM, and employing advanced methods such as SPA to extract characteristic wavelengths, they constructed multiple linear regression (MLR) models. Among these, the SPA-MLR model performed exceptionally well (Rp = 0.859, RMSEP = 38.789). This technology’s key contribution lies in enabling visualized detection of pesticide residue distribution, offering a novel technical approach for real-time monitoring in agricultural production [26].

Ma et al. proposed a non-destructive method for detecting pesticide residues on cantaloupe surfaces based on short-wave infrared HSI (SWIR-HSI, 1000–2500 nm) and an adaptive t-distribution honey badger algorithm-optimized extreme learning machine (tHBA-ELM). By comparing three models—ELM, SVM, and PLS-DA—they found that ELM achieved the highest accuracy (79.5%) in identifying five pesticide types, including acetamiprid and malathion. After normalization (NM) preprocessing, accuracy improved to 82%. The study innovatively applied the tHBA algorithm to optimize ELM parameters, enhancing population diversity through adaptive t-distribution mutation. This resulted in a test set accuracy of 93.5%, precision of 93.73%, and F1-score of 0.9355 for the tHBA-ELM model, outperforming GA-ELM (88.5%) and HBA-ELM (90.5%). Experimental results indicated that the SWIR band is sensitive to organic pesticides due to vibrational characteristics of C-H and O-H bonds, with the highest recognition rates for acetamiprid and difenoconazole (95%), while slightly lower for cypermethrin (92.5%) due to its volatility. This method provides an efficient, non-destructive solution for pesticide detection on thick-skinned fruits and vegetables, though model parameters need to be tailored to different pesticides and cultivars to improve generalization [154].

As research advances, scientists are increasingly exploring detection strategies for more complex scenarios. The need to detect mixed pesticide residues has further driven the development of HSI technology. Sun et al. demonstrated outstanding performance in detecting mixed pesticide residues on lettuce leaves by integrating hyperspectral sensing with imaging capabilities. This technique not only simultaneously acquires spectral and spatial information from samples but also enables precise selection of characteristic wavelengths through algorithms such as Competitive Adaptive Reweighted Sampling (CARS) and Recursive Feature Elimination based on Random Forest (RF-RFE). By establishing a Least Squares Support Vector Regression (LSSVR) model and simplifying it with the Successive Projections Algorithm (SPA), detection efficiency was significantly enhanced. The high efficiency and accuracy of this non-destructive method represent a revolutionary technological upgrade for monitoring systems of agricultural product quality and safety [27].

Furthermore, the integration of deep learning methods with hyperspectral data has enabled simultaneous identification of multiple mixed pesticides, achieving classification accuracies exceeding 92%. Xu et al. employed both visible/NIR (Vis-NIR) (376–1044 nm) and NIR (915–1699 nm) HSI systems (HIS) to detect pesticide residue levels. Three different grape varieties were sprayed with four levels of pesticide application. Classification models for pesticide residue levels were developed using Logistic Regression (LR), Support Vector Machine (SVM), Random Forest (RF), Convolutional Neural Network (CNN), and Residual Neural Network (ResNet). Significance maps from CNN and ResNet were used to visualize the contribution of different wavelengths. Overall, results obtained using NIR spectroscopy outperformed those from Vis-NIR. For Vis-NIR data, ResNet delivered the best performance, achieving an accuracy over 93%. For NIR data, LR performed best with accuracy exceeding 97%, although SVM, CNN, and ResNet also yielded close and robust results. The significance maps of CNN and ResNet revealed similar and consistent key wavelength ranges. These results indicate that deep learning models generally outperform traditional machine learning approaches. The study demonstrates that combining HSI with machine learning enables effective detection of pesticide residue levels in grapes [155].

Liu et al. developed a rapid, non-destructive method for detecting early herbicide stress in wheat seedlings by combining visible/NIR HSI (Vis/NIR HSI) with a shallow convolutional neural network (SCNN) (Figure 5). Two wheat cultivars (HM-920 and XN-20) were grown in a greenhouse to the three-leaf stage and then treated with three herbicides—56% MCPA-Na, mesosulfuron-methyl, and isoproturon—at varying concentration gradients (33%, 67%, and 100% of the recommended dose). Hyperspectral data (400–1000 nm) were collected from the leaves using a HSI system. First-derivative analysis and the SCNN-ATT model were applied for feature extraction and classification. Results showed that spectral differences were primarily concentrated in the 518–531 nm (carotenoids), 637–675 nm (chlorophyll), and red-edge regions (around 700 nm). The SCNN-ATT model achieved a 96% accuracy in classifying herbicide types and approximately 80% accuracy in classifying stress levels within 48 hours post-treatment. After selecting 15 key wavelengths using SCNN-FS (Feature Selection), the model maintained high accuracy, demonstrating the method's capability for non-destructive identification of early herbicide stress and providing a technical foundation for real-time, in-field monitoring [156].

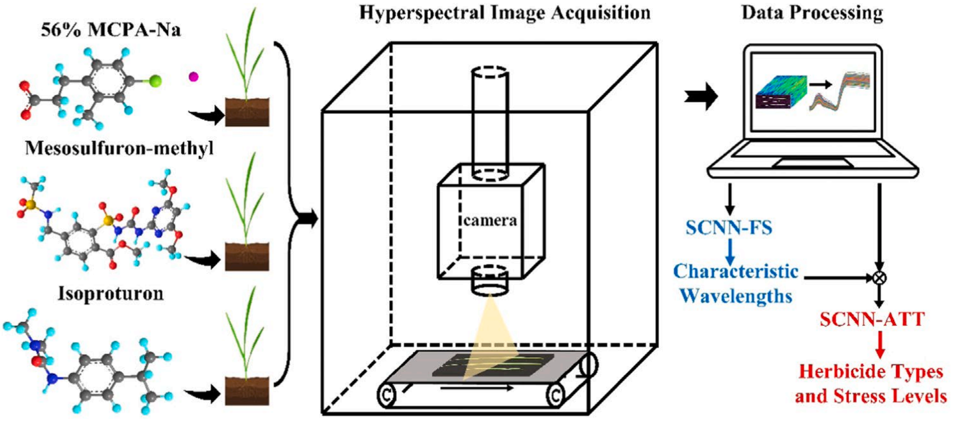

**Figure 5.** HSI of shallow convolutional neural network (SCNN) for predicting early herbicides in wheat varieties [156].

The ultimate goal of technological breakthroughs is to translate laboratory achievements into real-world applications. Researchers are increasingly focusing on how to move these advanced technologies out of the lab and into broader market use. In applied research within the 950–1650 nm spectral range, Ge et al. achieved a significant advancement by employing NIR transmittance spectroscopy. By combining SG-SNV (Savitzky-Golay smoothing and Standard Normal Variate) preprocessing with CARS-IRIV (CARS and Iteratively Retains Informative Variables) feature selection, and using a Grey Wolf Optimizer (GSA)-optimized Support Vector Machine (SVM) model, the method achieved 100% accuracy in qualitative detection of fenvalerate and 98.33% accuracy for chlorpyrifos. This study not only validated the reliability of the technology but, more importantly, provided a practical and feasible technical pathway for developing portable pesticide residue detection devices, signaling a new era of opportunities in the field of food safety inspection [157].

## 3. Research Limitations and Future Directions of Spectroscopic Techniques

Although spectroscopic techniques have demonstrated significant advantages in pesticide detection, several critical limitations remain. HSI can capture rich spatial-spectral information, but its data processing is highly complex and significantly affected by ambient lighting conditions, resulting in insufficient stability for practical field applications. SERS offers excellent sensitivity; however, the reproducibility and uniformity of substrate fabrication remain major challenges. Enhancement factors can vary by orders of magnitude between different substrate batches, severely compromising the reliability of quantitative analysis [158,159]. Fluorescence spectroscopy faces interference from endogenous fluorophores, particularly natural pigments such as chlorophyll, which can mask the characteristic signals of target pesticides [160]. All three techniques share common challenges: incomplete standard reference material systems leading to poor transferability of quantitative models; lack of standardized sample pre-treatment methods for complex agricultural matrices; and insufficient research on their adaptability to emerging pesticide types, such as bio-pesticides and nano-pesticides.

Future breakthroughs should focus on integrating technological innovation with engineering applications. For hyperspectral technology, developing adaptive illumination compensation models using deep learning algorithms and integrating miniaturized spectrometers could enable real-time field detection. In SERS, advancing controllable self-assembly processes for substrate fabrication and combining them with microfluidic chips could standardize detection workflows. Fluorescence spectroscopy could improve selectivity through the development of specific fluorescent probes (e.g., MIPs) and eliminate background interference using time-resolved fluorescence techniques. The synergistic use of these techniques also holds great potential—for example, a multi-level detection system combining HSI for rapid screening followed by SERS for confirmation. Furthermore, it is essential to establish comprehensive spectral databases covering major agricultural products, develop low-cost portable detection devices, and explore the application of blockchain technology for traceability of detection data. These efforts will ultimately create complete technical solutions bridging the gap from laboratory research to field deployment.

## 4. Conclusions

Spectroscopic techniques have evolved into a multi-layered technological framework for pesticide residue detection, with distinct application scenarios and performance advantages. SERS, leveraging plasmonic enhancement from nanomaterials and the development of portable devices, has become the preferred method for rapid on-site screening of trace pesticides—particularly suitable for the field detection of organophosphorus compounds. Attenuated total reflection infrared (ATR-IR) spectroscopy and fluorescence spectroscopy excel in laboratory settings: ATR-IR enhances selectivity toward carbamate pesticides via surface enhancement strategies, while fluorescence spectroscopy enables simultaneous identification of multiple pesticide residues in complex matrices using NIR fluorescent probes. UV-Vis derivatization colorimetric methods, valued for their low cost, support routine testing in grassroots laboratories. HSI, by fusing spatial and spectral information, can visually map the distribution patterns of pesticide residues on produce such as strawberries. Nanomaterials, serving as key enhancing substrates, have significantly improved the sensitivity and selectivity of these detection methods. However, current technologies still face bottlenecks including insufficient stability of nanomaterials, limited coverage of standard spectral libraries, and the complexity of multi-technique integration.Future research should prioritize three key directions: First, developing intelligent responsive nanosubstrates to enhance the reproducibility of SERS in complex environments. Second, constructing cross-modal spectral databases integrated with deep learning to enable rapid identification of unknown pesticides. Third, advancing the miniaturization of spectroscopy-MS (e.g., SERS-MS or HSI-MS) hybrid instruments to create seamless detection chains—from on-site screening to laboratory confirmation. These innovations will significantly improve the efficiency of agricultural product quality and safety monitoring, reduce non-point source pollution in agriculture through precise application guidance, and provide robust technological support for sustainable and green agriculture.

**Author Contributions:** Conceptualization, M.W. and X.S.; methodology, Q.B.; investigation, Y.N., H.P., and P.Z.; writing—review and editing, M.W. and X.S.; project administration, S.Y.; funding acquisition, M.W. All authors have read and agreed to the published version of the manuscript.

**Funding:** This research was funded by the National Natural Science Foundation of China, grant number 21905117.

**Data Availability Statement:** Not applicable.

**Conflicts of Interest:** The authors declare no conflicts of interest.

## References

1. Gao, Q.; Wang, Y.; Li, Y.; Yang, W.; Jiang, W.; Liang, Y.; Zhang, Z. Residue behaviors of six pesticides during apple juice production and storage. *Food Res. Int.* **2024,** *177*, 113894.
2. Zhang, Z.; Zhang, Y.; Jayan, H.; Gao, S.; Zhou, R.; Yosri, N.; Zou, X.; Guo, Z. Recent and emerging trends of metal-organic frameworks (MOFs)-based sensors for detecting food contaminants: A critical and comprehensive review. *Food Chem.* **2024,** *448*, 139051.
3. Duan, J.; Gao, Q.; Shi, L.; Li, Y.; Zhang, Z.; Liang, Y. Residue changes of five pesticides during the production and storage of rice flour. *Food Addit. Contam., Part A* **2022,** *39* (3), 542-550.
4. Liao, J.; Tao, W.; Liang, Y.; He, X.; Wang, H.; Zeng, H.; Wang, Z.; Luo, X.; Sun, J.; Wang, P.; Zang, Y. Multi-scale monitoring for hazard level classification of Brown Planthopper damage in rice using hyperspectral technique. *Int. J. Agric. Biol. Eng.* **2024,** *17* (6), 202-211.
5. Zhang, J.; Dai, L.; Huang, Z.; Gong, C.; Chen, J.; Xie, J.; Qu, M. Corn Seed Quality Detection Based on Spectroscopy and Its Imaging Technology: A Review. *Agriculture* **2025,** *15* (4), 390.
6. Wu, Z.; Ye, C.; Ye, Z.; Zhang, X.; Zhang, Q.; Zhang, Y.; Zhou, J.; Su, H. E. M.; Chen, X.; Su, T.; Yu, J.; Qian, X. Discovery of Enantiopure (S)-Methoprene Derivatives as Potent Biochemical Pesticide Candidates. *Adv. Funct. Mater.* **2024,** *72* (45), 24979-24988.
7. Yu, Y.; Wang, Y.; Okonkwo, C. E.; Chen, L.; Zhou, C. Multimode ultrasonic-assisted decontamination of fruits and vegetables: A review. *Food Chem.* **2024,** *450*, 139356.
8. Shoaib, M.; Li, H.; Zareef, M.; Khan, I. M.; Iqbal, M. W.; Niazi, S.; Raza, H.; Yan, Y.; Chen, Q. Recent Advances in Food Safety Detection: Split Aptamer-Based Biosensors Development and Potential Applications. *J. Agric. Food. Chem.* **2025,** *73* (8), 4397-4424.
9. Faye, C.; Bodian, E. H. T.; Thiaré, D. D.; Diouf, D.; Diop, N. A.; Bakhoum, J.-P.; Cisse, L.; Diaw, P. A.; Coly, A.; Giamarchi, P. Development of a new spectral database of photo-induced pesticide compounds for an automatic monitoring and identification system. *Anal. Chim. Acta* **2025,** *1335*, 343475.
10. Song, S.; Gao, Z.; Guo, X.; Chen, G. Aptamer-Based Detection Methodology Studies in Food Safety. *Food Anal. Methods* **2019,** *12* (4), 966-990.
11. Dai, Y.; Peng, W.; Ji, Y.; Wei, J.; Che, J.; Huang, Y.; Huang, W.; Yang, W.; Xu, W. A self-powered photoelectrochemical aptasensor using 3D-carbon nitride and carbon-based metal-organic frameworks for high-sensitivity detection of tetracycline in milk and water. *J. Food Sci.* **2024,** *89* (11), 8022-8035.
12. Marimuthu, M.; Xu, K.; Song, W.; Chen, Q.; Wen, H. Safeguarding food safety: Nanomaterials-based fluorescent sensors for pesticide tracing. *Food Chem.* **2025,** *463*, 141288.
13. Nguyen, D. H. H.; Muthu, A.; Elsakhawy, T.; Sheta, M. H.; Abdalla, N.; El-Ramady, H.; Prokisch, J. Carbon Nanodots-Based Sensors: A Promising Tool for Detecting and Monitoring Toxic Compounds. *Nanomater.* **2025,** *15* (10), 725.

14. Azam, S. M. R.; Ma, H.; Xu, B.; Devi, S.; Stanley, S. L.; Siddique, M. A. B.; Mujumdar, A. S.; Zhu, J. Multi-frequency multi-mode ultrasound treatment for removing pesticides from lettuce (Lactuca sativa L.) and effects on product quality. *Lwt* **2021,** *143*, 111147.
15. Yang, N.; Zhou, X.; Yu, D.; Jiao, S.; Han, X.; Zhang, S.; Yin, H.; Mao, H. Pesticide residues identification by impedance time-sequence spectrum of enzyme inhibition on multilayer paper-based microfluidic chip. *J. Food Process Eng.* **2020,** *43* (12), 13544.
16. Wu, X.; Zhang, T.; Wu, B.; Zhou, H. Identification of lambda-cyhalothrin residues on Chinese cabbage using fuzzy uncorrelated discriminant vector analysis and MIR spectroscopy. *Int. J. Agric. Biol. Eng.* **2022,** *15* (3), 217-224.
17. Xin, Z.; Jun, S.; Bing, L.; Xiaohong, W.; Chunxia, D.; Ning, Y. Study on pesticide residues classification of lettuce leaves based on polarization spectroscopy. *J. Food Process Eng.* **2018,** *41* (8), 12903.
18. Lee, H.; Liao, J.-D.; Sivashanmugan, K.; Liu, B. H.; Fu, W.-e.; Chen, C.-C.; Chen, G. D.; Juang, Y.-D. Gold Nanoparticle-Coated ZrO2-Nanofiber Surface as a SERS-Active Substrate for Trace Detection of Pesticide Residue. *Nanomater.* **2018,** *8* (6), 402.
19. Wang M.; Liu Z.; Yang F.; Bu Q.; Song X.; Yuan S. Multimodal Fusion-Driven Pesticide Residue Detection: Principles, Applications, and Emerging Trends. *Nanomater.* **2025,** *15*, 1305.
20. Yang, C.; Guo, Z.; Fernandes Barbin, D.; Dai, Z.; Watson, N.; Povey, M.; Zou, X. Hyperspectral Imaging and Deep Learning for Quality and Safety Inspection of Fruits and Vegetables: A Review. *J. Agric. Food. Chem.* **2025,** *73* (17), 10019-10035.
21. Li, Q.; Yang, Y.; Tan, M.; Xia, H.; Peng, Y.; Fu, X.; Huang, Y.; Yang, X.; Ma, X. Rapid pesticide residues detection by portable filter-array hyperspectral imaging. *Spectrochim. Acta, Part A* **2025,** *330*, 125703.
22. Liu, S.; Nie, C.; He, F.; Wu, G.; Wang, H.; Li, S.; Du, C.; Zheng, Z.; Cheng, J.; Shen, Y.; Cheng, J. Oxidase-like nanozymes-driven colorimetric, fluorescence and electrochemiluminescence assays for pesticide residues. *Trends Food Sci. Technol.* **2024,** *150*, 104597.
23. Xi, Q.; Chen, Q.; Ahmad, W.; Pan, J.; Zhao, S.; Xia, Y.; Ouyang, Q.; Chen, Q. Quantitative analysis and visualization of chemical compositions during shrimp flesh deterioration using hyperspectral imaging: A comparative study of machine learning and deep learning models. *Food Chem.* **2025,** *481*, 143997.
24. Tian, J.; Xu, S.; Wu, Y.; Shi, Y.; Duan, Y.; Li, Z.; Cao, H.; Zeng, J.; Shen, T.; Pan, L.; Xin, Z.; Fang, W.; Zhu, X. Authenticating vintage in white tea: Appearance-taste-aroma-based three-in-one non-invasive anticipation. *Food Res. Int.* **2025,** *199*, 115394.
25. Shen, Y.; Wu, X.; Wu, B.; Tan, Y.; Liu, J. Qualitative Analysis of Lambda-Cyhalothrin on Chinese Cabbage Using Mid-Infrared Spectroscopy Combined with Fuzzy Feature Extraction Algorithms. *Agric.* **2021,** *11* (3), 275.
26. Jiang, S.; Sun, J.; Xin, Z.; Mao, H.; Wu, X.; Li, Q. Visualizing distribution of pesticide residues in mulberry leaves using NIR hyperspectral imaging. *J. Food Process Eng.* **2016,** *40*, 12510.
27. Sun, J.; Cong, S.; Mao, H.; Wu, X.; Yang, N. Quantitative detection of mixed pesticide residue of lettuce leaves based on hyperspectral technique. *J. Food Process Eng.* **2017,** *41* (2), 12654.
28. Yang, N.; Tao, S.; Mao, H.; Wei, M.; Fu, J.; Song, W. An Integrated Platform and Method for Rapid High-Throughput Quantitative Detection of Organophosphorus Pesticide Residues. *IEEE Trans. Instrum. Meas.* **2024,** *73*, 9511011.
29. Johnson, N. A. N.; Adade, S. Y.-S. S.; Ekumah, J.-N.; Kwadzokpui, B. A.; Xu, J.; Xu, Y.; Chen, Q. A comprehensive review of analytical techniques for spice quality and safety assessment in the modern food industry. *Crit. Rev. Food Sci. Nutr.* **2025**, 1-26.
30. Bērziņš, K.; Sales, R. E.; Barnsley, J. E.; Walker, G.; Fraser-Miller, S. J.; Gordon, K. C. Low-wavenumber Raman spectral database of pharmaceutical excipients. *Vib. Spectrosc.* **2020,** *107*, 103021.
31. Dias, L. A. F.; Jussiani, E. I.; Appoloni, C. R. Reference Raman Spectral Database of Commercial Pesticides. *J. Appl. Spectrosc.* **2019,** *86* (1), 166-175.
32. Zhou, X.; Fang, Y.; Zhang, P. Raman Spectra of Pesticides on the Surface of Fruits. *J. Light Scattering*. **2004,** *16*, 11-14.

33. Shi, G.; Shen, X.; Ren, H.; Rao, Y.; Weng, S.; Tang, X. Kernel principal component analysis and differential non-linear feature extraction of pesticide residues on fruit surface based on surface-enhanced Raman spectroscopy. *Front. Plant Sci.* **2022,** *13*, 956778.
34. Xue, Y.; Jiang, H. Monitoring of Chlorpyrifos Residues in Corn Oil Based on Raman Spectral Deep-Learning Model. *Foods* **2023,** *12* (12), 2402.
35. Kuo, P.-H.; Chang, C.-W.; Tseng, Y.-R.; Yau, H.-T. Efficient, automatic, and optimized portable Raman-spectrum-based pesticide detection system. *Spectrochim. Acta, Part A* **2024,** *308*, 123787.
36. Yosri, N.; Gao, S.; Zhou, R.; Wang, C.; Zou, X.; El-Seedi, H. R.; Guo, Z. Innovative quantum dots-based SERS for ultrasensitive reporting of contaminants in food: Fundamental concepts and practical implementations. *Food Chem.* **2025,** *467*, 142395.
37. Liu, Z.; Yang, R.; Chen, H.; Zhang, X. Recent Advances in Food Safety: Nanostructure-Sensitized Surface-Enhanced Raman Sensing. *Foods* **2025,** *14* (7), 1115.
38. Jayan, H.; Zhou, R.; Zheng, Y.; Xue, S.; Yin, L.; El-Seedi, H. R.; Zou, X.; Guo, Z. Microfluidic-SERS platform with in-situ nanoparticle synthesis for rapid E. coli detection in food. *Food Chem.* **2025,** *471*, 142800.
39. Hassan, M. M.; Zareef, M.; Xu, Y.; Li, H.; Chen, Q. SERS based sensor for mycotoxins detection: Challenges and improvements. *Food Chem.* **2021,** *344*, 128652.
40. Sitjar, J.; Liao, J.-D.; Lee, H.; Liu, B. H.; Fu, W.-e. SERS-Active Substrate with Collective Amplification Design for Trace Analysis of Pesticides. *Nanomater.* **2019,** *9* (5), 664.
41. Ashiagbor, K.; Jayan, H.; Yosri, N.; Amaglo, N. K.; Zou, X.; Guo, Z. Advancements in SERS based systematic evolution of ligands by exponential enrichment for detection of pesticide residues in fruits and vegetables. *Food Chem.* **2025,** *463*, 141394.
42. Wei, W.; Hassan, M. M.; Wu, J.; Mu, X.; Li, H.; Chen, Q. Competitive Ratiometric Aptasensing with Core-Internal Standard-Shell Structure Based on Surface-Enhanced Raman Scattering. *J. Agric. Food. Chem.* **2022,** *71* (1), 857-866.
43. Guo, Z.; Wu, X.; Jayan, H.; Yin, L.; Xue, S.; El-Seedi, H. R.; Zou, X. Recent developments and applications of surface enhanced Raman scattering spectroscopy in safety detection of fruits and vegetables. *Food Chem.* **2024,** *434*, 137469.
44. Zhu, J.; Qian, H.; Zhu, A.; Guo, Z.; Chen, Q.; Xu, Y. Au octahedrons monolayer film SERS substrate coupled with a hybrid metaheuristic algorithm-optimized ELM model: An analytical strategy for rapid and label-free detection of zearalenone in corn oil. *Food Chem.* **2025,** *476*, 143516.
45. Yang, N.; Wang, P.; Xue, C. Y.; Sun, J.; Mao, H. P.; Oppong, P. K. A portable detection method for organophosphorus and carbamates pesticide residues based on multilayer paper chip. *J. Food Process Eng.* **2018,** *41* (8), 12867
46. Yang, H.; Qian, H.; Xu, Y.; Zhai, X.; Zhu, J. A Sensitive SERS Sensor Combined with Intelligent Variable Selection Models for Detecting Chlorpyrifos Residue in Tea. *Foods* **2024,** *13* (15), 2363.
47. Aheto, J. H.; Huang, X.; Tian, X.; Zhang, X.; Zhang, W.; Yu, S. Activated carbon@silver nanoparticles conjugates as SERS substrate for capturing malathion analyte molecules for SERS detection. *J. Food Saf.* **2023,** *43* (5), 13072.
48. Yang, S.; Yao, J.; Quan, Y.; Hu, M.; Su, R.; Gao, M.; Han, D.; Yang, J. Monitoring the charge-transfer process in a Nd-doped semiconductor based on photoluminescence and SERS technology. *Light Sci. Appl.* **2020,** *9* (1), 117.
49. Guo, Z.; Chen, P.; Yosri, N.; Chen, Q.; Elseedi, H. R.; Zou, X.; Yang, H. Detection of Heavy Metals in Food and Agricultural Products by Surface-enhanced Raman Spectroscopy. *Food Rev. Int.* **2021,** *39*, 1440-1461.
50. Hou, Y.; Zhang, Y.; Huang, Y.; Zhou, A.; Han, J.; Yang, K.; Zhao, Y.; Zhou, J.; Wang, J.; Chen, G.; Xu, X.; Xu, D.; Lv, J.; Chen, J.; Lv, H.; Liu, G. L. A pH-responsive MOFs@ MPN nanocarrier with enhancing antifungal activity for sustainable controlling myclobutanil release. *Chem. Eng. J.* **2024,** *497*, 155713.
51. Wang, M.; Shi, G.; Zhu, Y.; Wang, Y.; Ma, W. Au-Decorated Dragonfly Wing Bioscaffold Arrays as Flexible Surface-Enhanced Raman Scattering (SERS) Substrate for Simultaneous Determination of Pesticide Residues. *Nanomater.* **2018,** *8* (5), 289.

52. Chen, Z.; Sun, Y.; Zhang, X.; Shen, Y.; Khalifa, S. A. M.; Huang, X.; Shi, J.; Li, Z.; Zou, X. Green and sustainable self-cleaning flexible SERS base: Utilized for cyclic-detection of residues on apple surface. *Food Chem.* **2024,** *441*, 138345.
53. Li, H.; Mehedi Hassan, M.; Wang, J.; Wei, W.; Zou, M.; Ouyang, Q.; Chen, Q. Investigation of nonlinear relationship of surface enhanced Raman scattering signal for robust prediction of thiabendazole in apple. *Food Chem.* **2021,** *339*, 127843.
54. Park, J.; Kim, J.; Kim, J.; Kim, K.; Kim, J.; You, J.; Kim, D. W.; Kim, J. Highly sensitive thin SERS substrate by sandwich nanoarchitecture using multiscale nanomaterials for pesticide detection on curved surface of fruit. *J. Hazard. Mater.* **2025,** *494*, 138450.
55. Li, H.; Geng, W.; Hassan, M. M.; Zuo, M.; Wei, W.; Wu, X.; Ouyang, Q.; Chen, Q. Rapid detection of chloramphenicol in food using SERS flexible sensor coupled artificial intelligent tools. *Food Control* **2021,** *128*, 108186.
56. Sun, Y.; Zhai, X.; Xu, Y.; Liu, C.; Zou, X.; Li, Z.; Shi, J.; Huang, X. Facile fabrication of three-dimensional gold nanodendrites decorated by silver nanoparticles as hybrid SERS-active substrate for the detection of food contaminants. *Food Control* **2021,** *122*, 107772.
57. Pan, H.; Ahmad, W.; Jiao, T.; Zhu, A.; Ouyang, Q.; Chen, Q. Label-free Au NRs-based SERS coupled with chemometrics for rapid quantitative detection of thiabendazole residues in citrus. *Food Chem.* **2022,** *375*, 131681.
58. Ma, L.; Han, E.; Yin, L.; Xu, Q.; Zou, C.; Bai, J.; Wu, W.; Cai, J. Simultaneous detection of mixed pesticide residues based on portable Raman spectrometer and Au@Ag nanoparticles SERS substrate. *Food Control* **2023,** *153*, 109951.
59. Li, H.; Hu, W.; Hassan, M. M.; Zhang, Z.; Chen, Q. A facile and sensitive SERS-based biosensor for colormetric detection of acetamiprid in green tea based on unmodified gold nanoparticles. *J. Food Meas. Charact.* **2018,** *13* (1), 259-268.
60. Hassan, M. M.; Zareef, M.; Jiao, T.; Liu, S.; Xu, Y.; Viswadevarayalu, A.; Li, H.; Chen, Q. Signal optimized rough silver nanoparticle for rapid SERS sensing of pesticide residues in tea. *Food Chem.* **2021,** *338*, 127796.
61. Jiao, T.; Mehedi Hassan, M.; Zhu, J.; Ali, S.; Ahmad, W.; Wang, J.; Lv, C.; Chen, Q.; Li, H. Quantification of deltamethrin residues in wheat by Ag@ZnO NFs-based surface-enhanced Raman spectroscopy coupling chemometric models. Food Chem. 2021, 337, 127652.
62. Aheto, J. H.; Huang, X.; Wang, C.; Tian, X.; Yi, R.; Yuena, W. Fabrication and evaluation of chitosan modified filter paper for chlorpyrifos detection in wheat by surface-enhanced Raman spectroscopy. J. Sci. Food Agric. 2022, 102 (15), 7323-7330.
63. Wang, T.; Ji, B.; Cheng, Z.; Chen, L.; Luo, M.; Wei, J.; Wang, Y.; Zou, L.; Liang, Y.; Zhou, B.; Li, P. Semi-wrapped gold nanoparticles for surface-enhanced Raman scattering detection. Biosens. Bioelectron. 2023, 228, 115191.
64. Adade, S. Y.-S. S.; Lin, H.; Johnson, N. A. N.; Afang, Z.; Chen, Z.; Haruna, S. A.; Ekumah, J.-N.; Agyekum, A. A.; Li, H.; Chen, Q. Rapid quantitative analysis of acetamiprid residue in crude palm oil using SERS coupled with random frog (RF) algorithm. J. Food Compos. Anal. 2024, 125, 105818.
65. Torović, L.; Vuković, G.; Dimitrov, N. Pesticide residues in fruit juice in Serbia: Occurrence and health risk estimates. *J. Food Compos. Anal.* **2021,** *99*, 103889.
66. Sun, G.; Li, N.; Wang, D.; Xu, G.; Zhang, X.; Gong, H.; Li, D.; Li, Y.; Pang, H.; Gao, M.; Liang, X. A Novel 3D Hierarchical Plasmonic Functional Cu@Co3O4@Ag Array as Intelligent SERS Sensing Platform with Trace Droplet Rapid Detection Ability for Pesticide Residue Detection on Fruits and Vegetables. *Nanomater.* **2021,** *11* (12), 3460.
67. Ma, L.; Yang, X.; Yin, L.; Han, E.; Wang, C.; Zhou, R.; Bai, J.; Wang, Y.; Guo, Z.; Cai, J. Rapid dual-modal detection of two types of pesticides in fruits using SERS-based immunoassay. *J. Food Compos. Anal.* **2024,** *136*, 106781.
68. Zheng, Y.; Yin, L.; Jayan, H.; Jiang, S.; El-Seedi, H. R.; Zou, X.; Guo, Z. In situ self-cleaning PAN/Cu2O@Ag/Au@Ag flexible SERS sensor coupled with chemometrics for quantitative detection of thiram residues on apples. *Food Chem.* **2025,** *473*, 143032.

69. Tao, M.; Fang, H.; Feng, X.; He, Y.; Liu, X.; Shi, Y.; Wei, Y.; Hong, Z.; Fan, Y. Rapid Trace Detection of Pesticide Residues on Tomato by Surface-Enhanced Raman Spectroscopy and Flexible Tapes. *J. Food Qual.* **2022,** *2022*, 6947775.
70. Chen, Z.; Sun, Y.; Shi, J.; Zhang, W.; Zhang, X.; Hang, X.; Li, Z.; Zou, X. Convenient self-assembled PDADMAC/PSS/Au@Ag NRs filter paper for swift SERS evaluate of non-systemic pesticides on fruit and vegetable surfaces. *Food Chem.* **2023,** *424*, 136232.
71. Alsammarraie, F. K.; Lin, M. Using Standing Gold Nanorod Arrays as Surface-Enhanced Raman Spectroscopy (SERS) Substrates for Detection of Carbaryl Residues in Fruit Juice and Milk. *J. Agric. Food. Chem.* **2017,** *65*, 666-674.
72. Chen, Z.; Sun, Y.; Shi, J.; Zhang, W.; Zhang, X.; Huang, X.; Zou, X.; Li, Z.; Wei, R. Facile synthesis of Au@Ag core–shell nanorod with bimetallic synergistic effect for SERS detection of thiabendazole in fruit juice. *Food Chem.* **2022,** *370*, 131276.
73. Neo, E. R. K.; Low, J. S. C.; Goodship, V.; Debattista, K. Deep learning for chemometric analysis of plastic spectral data from infrared and Raman databases. *Resour. Conserv. Recycl.* **2023,** *188*, 106718.
74. Xu, Y.; Hassan, M. M.; Ali, S.; Li, H.; Ouyang, Q.; Chen, Q. Self-Cleaning-Mediated SERS Chip Coupled Chemometric Algorithms for Detection and Photocatalytic Degradation of Pesticides in Food. *J. Agric. Food. Chem.* **2021,** *69* (5), 1667-1674.
75. Zhu, A.; Xu, Y.; Ali, S.; Ouyang, Q.; Chen, Q. Au@Ag nanoflowers based SERS coupled chemometric algorithms for determination of organochlorine pesticides in milk. *Lwt* **2021,** *150*, 111978.
76. Zhu, J.; Agyekum, A. A.; Kutsanedzie, F. Y. H.; Li, H.; Chen, Q.; Ouyang, Q.; Jiang, H. Qualitative and quantitative analysis of chlorpyrifos residues in tea by surface-enhanced Raman spectroscopy (SERS) combined with chemometric models. *Lwt* **2018,** *97*, 760-769.
77. Li, H.; Luo, X.; Haruna, S. A.; Zareef, M.; Chen, Q.; Ding, Z.; Yan, Y. Au-Ag OHCs-based SERS sensor coupled with deep learning CNN algorithm to quantify thiram and pymetrozine in tea. *Food Chem.* **2023,** *428*, 136798.
78. Neng, J.; Wang, J.; Wang, Y.; Zhang, Y.; Chen, P. Trace analysis of food by surface-enhanced Raman spectroscopy combined with molecular imprinting technology: Principle, application, challenges, and prospects. *Food Chem.* **2023,** *429*, 136883.
79. arooq, S.; Chen, B.; Gao, F.; Muhammad, I.; Ahmad, S.; Wu, H. Development of Molecularly Imprinted Polymers for Fenthion Detection in Food and Soil Samples. *Nanomater.* **2022,** *12* (13), 2129.
80. Yang, Y.; Li, Y.; Zhai, W.; Li, X.; Li, D.; Lin, H.; Han, S. Electrokinetic Preseparation and Molecularly Imprinted Trapping for Highly Selective SERS Detection of Charged Phthalate Plasticizers. *Anal. Chem.* **2020,** *93* (2), 946-955.
81. Cao, X.; Hu, Y.; Yu, H.; Sun, S.; Xu, D.; Zhang, Z.; Cong, S.; She, Y. Detection of neonicotinoids in agricultural products using magnetic molecularly imprinted polymers-surface enhanced Raman spectroscopy. *Talanta* **2024,** *266*, 125000.
82. Neng, J.; Liao, C.; Wang, Y.; Wang, Y.; Yang, K. Rapid and Sensitive Detection of Pentachloronitrobenzene by Surface-Enhanced Raman Spectroscopy Combined with Molecularly Imprinted Polymers. *Biosensors* **2022,** *12*, 52.
83. Yan, M.; She, Y.; Cao, X.; Ma, J.; Chen, G.; Hong, S.; Shao, Y.; Abd El-Aty, A. M.; Wang, M.; Wang, J. A molecularly imprinted polymer with integrated gold nanoparticles for surface enhanced Raman scattering based detection of the triazine herbicides, prometryn and simetryn. *Microchim. Acta* **2019,** *186*, 143.
84. Xu, Y.; Hassan, M. M.; Ali, S.; Li, H.; Chen, Q. SERS-based rapid detection of 2,4-dichlorophenoxyacetic acid in food matrices using molecularly imprinted magnetic polymers. *Microchim. Acta* **2020,** *187*, 454.
85. Li, H.; Wang, Z.; Wang, X.; Jiang, J.; Xu, Y.; Liu, X.; Yan, Y.; Li, C. Preparation of a self-cleanable molecularly imprinted sensor based on surface-enhanced Raman spectroscopy for selective detection of R6G. *Anal. Bioanal. Chem.* **2017,** *409*, 4627-4635.
86. Hua, M. Z.; Feng, S.; Wang, S.; Lu, X. Rapid detection and quantification of 2,4-dichlorophenoxyacetic acid in milk using molecularly imprinted polymers–surface-enhanced Raman spectroscopy. *Food Chem.* **2018,** *258*, 254-259.

87. Liu, S.; Song, J.; Feng, S.; Li, J.; Wang, X.; Wang, X.; Wang, Y.; Liu, G. Composite Nanotube Arrays for Pesticide Detection Assisted with Machine Learning Based on SERS Effect. *ACS Appl. Nano Mater.* **2025,** *8* (18), 9544-9554.
88. Wang, H.-L.; You, E.-M.; Panneerselvam, R.; Ding, S.-Y.; Tian, Z.-Q. Advances of surface-enhanced Raman and IR spectroscopies: from nano/microstructures to macro-optical design. *Light Sci. Appl.* **2021,** *10* (1), 161.
89. Liu, L.; Zareef, M.; Wang, Z.; Li, H.; Chen, Q.; Ouyang, Q. Monitoring chlorophyll changes during Tencha processing using portable near-infrared spectroscopy. *Food Chem.* **2023,** *412*, 135505.
90. Haruna, S. A.; Ivane, N. M. A.; Adade, S. Y.-S. S.; Luo, X.; Geng, W.; Zareef, M.; Jargbah, J.; Li, H.; Chen, Q. Rapid and simultaneous quantification of phenolic compounds in peanut (Arachis hypogaea L.) seeds using NIR spectroscopy coupled with multivariate calibration. *J. Food Compos. Anal.* **2023,** *123*, 105516.
91. Wang, J.; Xie, Z.; Zhu, Y.; Zeng, P.; He, S.; Wang, J.; Wei, H.; Yu, C. Surface-enhanced infrared absorption spectroscopy (SEIRAS) for biochemical analysis: Progress and perspective. *Trends Environ. Anal. Chem.* **2024,** *41*, e00226.
92. Yu, G.; Ma, B.; Chen, J.; Li, X.; Li, Y.; Li, C. Nondestructive identification of pesticide residues on the Hami melon surface using deep feature fusion by Vis/NIR spectroscopy and 1D-CNN. *J. Food Process Eng.* **2020,** *44* (1), 13602.
93. Kesama, M. R.; Yan, F.; Zhang, R.; Wang, S.; Zhang, N.; Zhang, X. A pesticide residue detection model for food based on NIR and SERS. *Plos One* **2025,** *20*, e0320456.
94. Garrigues, S.; de la Guardia, M.; Cassella, A. R.; de Campos, R. C.; Santelli, R. E.; Cassella, R. J. Flow injection-FTIR determination of dithiocarbamate pesticides. *The Analyst* **2000,** *125*, 1829-1833.
95. Yang, X.; Sun, Z.; Low, T.; Hu, H.; Guo, X.; García de Abajo, F. J.; Avouris, P.; Dai, Q. Nanomaterial-Based Plasmon-Enhanced Infrared Spectroscopy. *Adv. Mater.* **2018,** *30* (20), 1704896.
96. Trindade, F. C. S.; de Souza Sobrinha, I. G.; Pereira, G.; Pereira, G. A. L.; Raimundo, I. M.; Pereira, C. F. A surface-enhanced infrared absorption spectroscopy (SEIRA) multivariate approach for atrazine detection. *Spectrochim. Acta, Part A* **2024,** *322*, 124867.
97. Jiang, X.; Shi, L.; Luo, B.; Wang, D.; Wang, Z.; Fan, M.; Gong, Z. *Spectroscopy and Spectral Analysis*. **2020**, *40*, 1809-1814.
98. Xing, J.; Zhao, C.; Zou, Y.; Kong, W.; Yu, Z.; Shan, Y.; Dong, Q.; Zhou, D.; Yu, W.; Guo, C. Modulating the optical and electrical properties of MAPbBr3 single crystals via voltage regulation engineering and application in memristors. *Light Sci. Appl.* **2020,** *9*, 111.
99. Gong, L.; Mo, Z. Based on the hybrid perovskite surface-enhanced IR research[D]. Chongqing: College of Chemistry and Chemical Engineering of Chongqing University, **2015**.
100. Shan, L.; Lv, J.; Liang, J.; Xu, J.; Wu, C.; Wang, A.; Zhang, L.; Ge, S.; Li, L.; Yu, J. Spin-State Reconfigurable Magnetic Perovskite-Based Photoelectrochemical Sensing Platform for Sensitive Detection of Acetamiprid. *Adv. Funct. Mater.* **2025**, 2418023.
101. Yang, Y.; Zhang, H.; Cai, W. Advances in Electrochemical Surface-Enhanced Infrared Spectroscopy. *Electrochemistry*. **2013**, *19*, 9-19.
102. Jiang, X.; Gong, Z.; Luo, B. Preparation of surface enhanced infrared absorption spectroscopy substrate and its application in rapid detection of DMDS pesticides[D]. Sichuan: Southwest Jiaotong University, **2013**.
103. Shi, L.; Sun, J.; Cong, S.; Ji, X.; Yao, K.; Zhang, B.; Zhou, X. Fluorescence hyperspectral imaging for detection of selenium content in lettuce leaves under cadmium-free and cadmium environments. *Food Chem.* **2025,** *481*, 144055.
104. Saleem, A.; Imtiaz, A.; Yaqoob, S.; Awais, M.; Awan, K. A.; Naveed, H.; Khalifa, I.; Al-Asmari, F.; Qian, J. Y. Integration of Fluorescence Spectroscopy Along with Mathematical Modeling for Rapid Prediction of Adulteration in Cooked Minced Beef Meat. *J. Food Process Eng.* **2024,** *47* (12).
105. Hu, T.; Xu, J.; Ye, Y.; Han, Y.; Li, X.; Wang, Z.; Sun, D.; Zhou, Y.; Ni, Z. Visual detection of mixed organophosphorous pesticide using QD-AChE aerogel based microfluidic arrays sensor. *Biosens. Bioelectron.* **2019,** *136*, 112-117.
106. Li, C.; Zhang, W.; Xu, X.; Zhou, L. Applications and Challenges of Fluorescent Probes for the Detection of Pesticide Residues in Food. *J. Agric. Food. Chem.* **2025,** *73*, 4982-4997.

107. Li, Q.; Hao, Z.; Zhang, C.; Ni, S.; Jiang, P.; Fan, P.; Li, L. Dual-Mode Detection of Glyphosate Based on DNAzyme-Mediated Click Chemistry and DNAzyme-Regulated CeO2 Peroxidase-like Activity. *J. Agric. Food. Chem.* **2025,** *73*, 7496-7503.
108. Gao, J.; Yang, X.; Liu, S.; Liu, Y.; Ning, X. Detection of Tomato Leaf Pesticide Residues Based on Fluorescence Spectrum and Hyper-Spectrum. *Hortic.* **2025,** *11* (2), 121.
109. Zhang, Y.; Hassan, M. M.; Rong, Y.; Liu, R.; Li, H.; Ouyang, Q.; Chen, Q. A solid-phase capture probe based on upconvertion nanoparticles and inner filter effect for the determination of ampicillin in food. *Food Chem.* **2022,** *386*, 132739.
110. Yin, L.; Hu, X.; Hao, M.; Shi, J.; Zou, X.; Dusabe, K. D. Upconversion nanoparticles-based background-free selective fluorescence sensor developed for immunoassay of fipronil pesticide. *J. Food Meas. Charact.* **2023,** *17* (3), 3125-3133.
111. Zhang, S.; Li, S.; Li, D.; Wu, J.; Jiao, T.; Wei, J.; Chen, X.; Chen, Q.; Chen, Q. Sulfadiazine detection in aquatic products using upconversion nanosensor based on photo-induced electron transfer with imidazole ligands and copper ions. *Food Chem.* **2024,** *456*, 139992.
112. Ma, L.; Yang, X.; Xue, S.; Zhou, R.; Wang, C.; Guo, Z.; Wang, Y.; Cai, J. "Raman plus X" dual-modal spectroscopy technology for food analysis: A review. *Compr. Rev. Food Sci. Food Saf.* **2025,** *24* (1), 70102.
113. Wang, J.; Wang, S.; Liu, N.; Shang, F. A detection method of two carbamate pesticides residues on tomatoes utilizing excitation-emission matrix fluorescence technique. *Microchem. J.* **2021,** *164*, 105920.
114. Luo, S.; Peng, R.; Wang, Y.; Liu, X.; Ren, J.; Li, W.; Xiong, Y.; Yi, S.; Wen, Q. Enzyme-targeted near-infrared fluorescent probe for organophosphorus pesticide residue detection. *Anal. Bioanal.Chem.* **2023,** *415* (20), 4849-4859.
115. Fan, C.; Wei, L.; Limeng, Y.; Li, Y.; Zheng, M.; Song, Y.; Shu, W.; Zeng, C. A novel ultrafast and highly sensitive NIR fluorescent probe for the detection of organophosphorus pesticides in foods and biological systems. *Food Chem.* **2025,** *463*, 141172.
116. Nekoueian, K.; Amiri, M.; Sillanpää, M.; Marken, F.; Boukherroub, R.; Szunerits, S. Carbon-based quantum particles: an electroanalytical and biomedical perspective. *Chem. Soc. Rev.* **2019,** *48* (15), 4281-4316.
117. Su, D.; Li, H.; Yan, X.; Lin, Y.; Lu, G. Biosensors based on fluorescence carbon nanomaterials for detection of pesticides. *TrAC, Trends Anal. Chem.* **2021,** *134*, 116126.
118. Xiao, H.; Li, P.; Tang, B. Recent progresses in fluorescent probes for detection of polarity. *Coord. Chem. Rev.* **2021,** *427*, 213582.
119. Xu, X.; Yan, B.; Lian, X. Wearable glove sensor for non-invasive organophosphorus pesticide detection based on a double-signal fluorescence strategy. *Nanoscale* **2018,** *10* (28), 13722-13729.
120. Liu, W.; Zhang, D.; Zhu, W.; Zhang, S.; Wang, Y.; Yu, S.; Liu, T.; Zhang, X.; Zhang, W.; Wang, J. Colorimetric and visual determination of total nereistoxin-related insecticides by exploiting a nereistoxin-driven aggregation of gold nanoparticles. *Microchim. Acta* **2015,** *182*, 401–408.
121. Han, A.; Hao, S.; Yang, Y.; Li, X.; Luo, X.; Fang, G.; Liu, J.; Wang, S. Perspective on recent developments of nanomaterial based fluorescent sensors: applications in safety and quality control of food and beverages. *J. Food Drug Anal.* **2020,** *28*, 487-508.
122. Marimuthu, M.; Arumugam, S. S.; Sabarinathan, D.; Li, H.; Chen, Q. Metal organic framework based fluorescence sensor for detection of antibiotics. *Trends Food Sci. Technol.* **2021,** *116*, 1002-1028.
123. Sun, Y.; Zhai, X.; Zou, X.; Shi, J.; Huang, X.; Li, Z. A Ratiometric Fluorescent Sensor Based on Silicon Quantum Dots and Silver Nanoclusters for Beef Freshness Monitoring. *Foods* **2023,** *12*, 1464.
124. Cao, J.; Wang, M.; Shao, Y.; She, Y.; Cao, Z.; Xiao, M.; Jin, F.; Wang, J.; Abd El-Aty, A. M. Fluorescent sensor for rapid detection of organophosphate pesticides using recombinant carboxylesterase PvCarE1 and glutathione-stabilized gold nanoclusters. *Microchemical Journal* **2024,** *200*, 110322.
125. Dong, J.; Yang, H.; Li, Y.; Liu, A.; Wei, W.; Liu, S. Fluorescence sensor for organophosphorus pesticide detection based on the alkaline phosphatase-triggered reaction. *Anal. Chim. Acta* **2020,** *1131*, 102-108.
126. Irshad, H.; Khadija; Qvortrup, K. Advances in fluorescent sensors for trace detection of metal contaminants and agrochemical residues in soil: A comprehensive review. *TrAC Trends Anal. Chem.* **2025,** *191*, 118365.

127. Wu, N.; Zhao, L.-X.; Jiang, C.-Y.; Li, P.; Liu, Y.; Fu, Y.; Ye, F. A naked-eye visible colorimetric and fluorescent chemosensor for rapid detection of fluoride anions: Implication for toxic fluorine-containing pesticides detection. *J. Mol. Liq.* **2020,** *302*, 112549.
128. Yang, J.; Chen, S.-W.; Zhang, B.; Tu, Q.; Wang, J.; Yuan, M.-S. Non-biological fluorescent chemosensors for pesticides detection. *Talanta* **2022,** *240*, 123200.
129. Li, M.; Wang, Z.; Tang, H.; Yang, J.; Luo, X.; Tian, Y.; Yang, M.; Jiang, J.; Wang, M.; Zheng, L.; Ma, C.; Xing, G.; Wang, H.; Li, J. A bionic palladium metal–organic framework based on a fluorescence sensing enhancement mechanism for sensitive detection of phorate. *Nanoscale* **2025,** *17* (2), 934-946.
130. Chen, M.-X.; Cheng, J.-H.; Ma, J.; Sun, D.-W. Advancing Aquatic Food Safety Detection Using Highly Sensitive Graphene Oxide and Reduced Graphene Oxide (GO/r-GO) Fluorescent Sensors. *Food Eng. Rev.* **2024,** *16* (4), 618-634.
131. Wang, Z.-P.; Wang, Y.; Li, X.-Y.; Jia, L.-F.; Yang, A.-Z.; Zhao, W.-T.; Jia, Y.; Yu, B.-Y.; Zhao, H.-Q. Water-stable mixed-ligand Cd(II) metal-organic frameworks as bis-color excited fluorescent sensors for the detection of vitamins and pesticides in aqueous solutions. *J. Mol. Struct.* **2024,** *1305*, 137699.
132. Gori, M.; Thakur, A.; Sharma, A.; Flora, S. J. S. Organic-Molecule-Based Fluorescent Chemosensor for Nerve Agents and Organophosphorus Pesticides. *Top. Curr. Chem.* **2021,** *379*, 33.
133. Feng, J.; Gong, Y.; Yang, S.; Qiu, G.; Tian, H.; Sun, B. Determination of carboxylesterase by fluorescence probe to guide detection of carbamate pesticide. *Luminescence* **2023,** *39* (1), 4625.
134. Ji, R.; Ma, S.; Yao, H.; Han, Y.; Yang, X.; Chen, R.; Yu, Y.; Wang, X.; Zhang, D.; Zhu, T.; Bian, H. Multiple kinds of pesticide residue detection using fluorescence spectroscopy combined with partial least-squares models. *Appl. Opt.* **2020,** *59*, 1524.
135. Lai, X.; Cao, W.; Zhang, G.; Ang, E. H.; Su, L.; Liu, C.; He, W.; Lai, W.; Deng, S. Traffic signal-inspired fluorescence lateral flow immunoassay utilizing self-assembled AIENP@Ni/EC for simultaneous multi-pesticide residue detection. *Chem. Eng. J.* **2024,** *501*, 157565.
136. Noori, Z.; de P. R. Moreira, I.; Bofill, J. M.; Poater, J. Adjusting UV-Vis Spectrum of Alizarin by Insertion of Auxochromes. *ChemistryOpen* **2024,** *13*, e202400030.
137. Abdolkarimi-Mahabadi, M.; Bayat, A.; Mohammadi, A. Use of UV-Vis Spectrophotometry for Characterization of Carbon Nanostructures: a Review. *Theor. Exp. Chem.* **2021,** *57* (3), 191-198.
138. Zhao, J.; Zhang, Y.; Yan, X.; Gan, L.; Wang, G. Investigation of UV-vis spectra of azobenzene containing carboxyl groups. *J. Mol. Model.* **2021,** *27* (3), 79.
139. Chen, D.; Liu, N.; Lin, W.; Chen, Z.; Lin, F.; Ma, Y.; Li, X.H. Determination of Orthophenylphenol in Tea by Ultraviolet Spectrophotometry. *Fujian Tea*, **2017**, *(12)*, 15-16.
140. Meng, D.; Yu, X.; Xu, L.; Zhang, W.; Zhao, Z. Simultaneous Detection of Imidacloprid, Acetamiprid, and Clothianidin in Apple Juice Using Ultraviolet Spectroscopy and the SSA–BPNN Model. *J. Appl. Spectrosc.* **2025,** *92* (2), 363-369.
141. Huang, G.; Cai, H.; Zeng, Q.; Ni, H. Study on an Alkalinehydrolysis-spectrophotometry for Detecting Organophosphate Pesticide. *J. Jimei University (Natural Science)*, **2009**, *14*, 17-22.
142. Gao, H.; Yang, P. Study on the determination of pesticide residues by pre-column fluorescence derivatization and high-performance liquid chromatography[D]. Sichuan: China West Normal University, **2016**.
143. Liu, A.; Zhang, Q.; Pan, L.; Yang, F.; Lin, D.; Jiang, C. Supramolecular Fluorescence Probe for Rapid Visual Detection of Pyrethroid and Composite Aerogel as a Pyrethroid Vapor Sensor. *Anal. Chem.* **2025,** *97* (25), 13672-13680.
144. Wang, P.; Li, H.; Hassan, M. M.; Guo, Z.; Zhang, Z.; Chen, Q. Fabricating an Acetylcholinesterase Modulated UCNPs-Cu2+ Fluorescence Biosensor for Ultrasensitive Detection of Organophosphorus Pesticides-Diazinon in Food. *J. Agric. Food. Chem.* **2019,** *67*, 8b07201.
145. Wang, F.; Zhu, Y.; Qian, L.; Yin, Y.; Yuan, Z.; Dai, Y.; Zhang, T.; Yang, D.; Qiu, F. Lamellar Ti3C2 MXene composite decorated with platinum-doped MoS2 nanosheets as electrochemical sensing functional platform for highly sensitive analysis of organophosphorus pesticides. *Food Chem.* **2024,** *459*, 140379.
146. Zhu, Y.; Wu, J.; Han, L.; Wang, X.; Li, W.; Guo, H.; Wei, H. Nanozyme Sensor Arrays Based on Heteroatom-Doped Graphene for Detecting Pesticides. *Anal. Chem.* **2020,** *92*, 9b05110.

147. Adade, S. Y.-S. S.; Lin, H.; Johnson, N. A. N.; Nunekpeku, X.; Aheto, J. H.; Ekumah, J.-N.; Kwadzokpui, B. A.; Teye, E.; Ahmad, W.; Chen, Q. Advanced food contaminant detection through multi-source data fusion: Strategies, applications, and future perspectives. *Trends Food Sci. Technol.* **2025,** *156*, 104851.
148. Xin, X.; Sun, J.; Shi, L.; Yao, K.; Zhang, B. Application of hyperspectral imaging technology combined with ECA-MobileNetV3 in identifying different processing methods of Yunnan coffee beans. *J. Food Compos. Anal.* **2025,** *143*, 107625.
149. Zhang, L.; Chen, M.; Duan, H.; Bu, Q.; Dong, X. Recent advances of optical sensors for point-of-care detection of phthalic acid esters. *Front. Sustainable Food Syst.* **2024,** *8*, 1474831.
150. Li, L.; Xie, S.; Ning, J.; Chen, Q.; Zhang, Z. Evaluating green tea quality based on multisensor data fusion combining hyperspectral imaging and olfactory visualization systems. *J. Sci. Food Agric.* **2018,** *99* (4), 1787-1794.
151. Sun, J.; Zhou, X.; Mao, H.; Wu, X.; Zhang, X.; Li, Q. Discrimination of pesticide residues in lettuce based on chemical molecular structure coupled with wavelet transform and near infrared hyperspectra. *J. Food Process Eng.* **2016,** *40* (4), 12509.
152. Wu, M.; Sun, J.; Lu, B.; Ge, X.; Zhou, X.; Zou, M. Application of deep brief network in transmission spectroscopy detection of pesticide residues in lettuce leaves. *J. Food Process Eng.* **2019,** *42* (3), 13005.
153. Sun, J.; Zhou, X.; Mao, H.; Wu, X.; Zhang, X.; Gao, H. Identification of pesticide residue level in lettuce based on hyperspectra and chlorophyll fluorescence spectra. *Int. J. Agric. Biol. Eng.* **2016,** *9*, 231-239.
154. Hu, Y.; Ma, B.; Wang, H.; Li, Y.; Zhang, Y.; Yu, G. Non-Destructive Detection of Different Pesticide Residues on the Surface of Hami Melon Classification Based on tHBA-ELM Algorithm and SWIR Hyperspectral Imaging. *Foods* **2023,** *12*, 1773.
155. Ye, W.; Yan, T.; Zhang, C.; Duan, L.; Chen, W.; Song, H.; Zhang, Y.; Xu, W.; Gao, P. Detection of Pesticide Residue Level in Grape Using Hyperspectral Imaging with Machine Learning. *Foods* **2022,** *11* (11), 1609.
156. Chu, H.; Zhang, C.; Wang, M.; Gouda, M.; Wei, X.; He, Y.; Liu, Y. Hyperspectral imaging with shallow convolutional neural networks (SCNN) predicts the early herbicide stress in wheat cultivars. *J. Hazard. Mater.* **2022,** *421*, 126706.
157. Sun, J.; Ge, X.; Wu, X.; Dai, C.; Yang, N. Identification of pesticide residues in lettuce leaves based on near infrared transmission spectroscopy. *J. Food Process Eng.* **2018,** *41* (6), 12816.
158. Bernat, A.; Samiwala, M.; Albo, J.; Jiang, X.; Rao, Q. Challenges in SERS-based pesticide detection and plausible solutions. *J. Agric. Food. Chem.* **2019,** *67* (45), 12341-12347.
159. Hu, J.; Zou, Y.; Sun, B.; Yu, X.; Shang, Z.; Huang, J.; Jin, S.; Liang, P. Raman spectrum classification based on transfer learning by a convolutional neural network: Application to pesticide detection. *Spectrochim. Acta, Part A* **2022,** *265*, 120366.
160. Zhang, L.; Sun, Y.; Zhang, Z.; Shen, Y.; Li, Y.; Ma, T.; Zhang, Q.; Ying, Y.; Fu, Y. Portable and durable sensor based on porous MOFs hybrid sponge for fluorescent-visual detection of organophosphorus pesticide. *Biosens. Bioelectron.* **2022,** *216*, 114659.